

## 9. Chromium 1994

David K. Geiger

### CONTENTS

INTRODUCTION .....	359
9.1 CHROMIUM(VI) .....	360
9.2 CHROMIUM(V) .....	361
9.3 CHROMIUM(IV) .....	361
9.4 CHROMIUM(III) .....	362
9.4.1 Complexes with monodentate ligands .....	362
9.4.2 Complexes with didentate ligands .....	364
9.4.2.1 Oxygen donor ligand systems .....	364
9.4.2.2 Nitrogen donor ligand systems .....	367
9.4.2.3 Sulfur donor ligand systems .....	369
9.4.2.4 Mixed donor ligand systems .....	370
9.4.3 Complexes with polydentate ligands .....	372
9.4.3.1 Tridentate ligands .....	372
9.4.3.2 Tetradentate ligands .....	374
9.4.3.3 Quinquedentate and sexidentate ligands .....	376
9.4.4 Complexes with macrocyclic ligands .....	376
9.4.5 Dinuclear complexes .....	378
9.4.6 Polynuclear complexes .....	381
9.5 CHROMIUM(II) .....	385
9.5.1 Mononuclear complexes .....	385
9.5.2 Dinuclear complexes .....	386
9.5.3 Polynuclear complexes .....	388
REFERENCES .....	388

### INTRODUCTION

This review covers the coordination chemistry of chromium published in 1994. Although not comprehensive, this review aims to provide a broad and representative survey of the literature of the period. Volumes 120 through 122 of *Chemical Abstracts*, *CARL UnCover Online*, and the indices of major journals in the area were used to obtain the citations included herein. In general, organometallic complexes are not covered. The organization used is similar to that employed in

previous years with particular emphasis placed on the ligand systems. The author is indebted to Sonia Landes, Reference Librarian, Milne Library, SUNY Geneseo for help with electronic literature searches.

A number of relevant review articles appeared in the literature during 1994. A review of the oxidation-reduction chemistry of chromium(IV) was published [1]. The coordination chemistry of chromium(III) cyano-am(m)ine complexes was reviewed [2]. In addition, a general review article on substitution reactions of chromium was published during this period [3].

### 9.1 CHROMIUM(VI)

In the reduction of chromium(VI) by glutathione, a relatively stable thioester intermediate is involved. The formation, decomposition, and reactivity of the chromium(VI) glutathione thioester intermediate was studied. The use of an exact integrated rate law allowed for the determination of the three rate constants from a single kinetic experiment [4,5].

A study of the oxidation of d-gluconic acid by chromium(VI) in perchloric acid leads to the formation of 2-ketogluconic acid. A build-up and decay of chromium(V) accompanies the loss of chromium(VI). The results suggest that C-H scission at the  $\alpha$ -carbon is preferred to C-C scission for the oxidation of gluconic acid [6].

The reaction between chromium(VI) and DL-penicillamine was examined from pH 1–8. The overall stoichiometry of the reaction, where RSH represents the penicillamine, is given in equation (i).



The process involves the formation of an intermediate thioester. The kinetics for the formation of the intermediate thioester was studied. A dependence on the nature and concentration of the buffer and electrolyte was found [7].

The oxidation of ethanol by (3,4-lutidine)(oxo)bis(peroxo)chromium(VI) to acetaldehyde was examined in dichloromethane solution. The reaction has a first-order dependence on oxidant and a one-half dependence on reactant. Activation parameters are reported [8].

A potentiometric and spectrophotometric study of the complexation equilibria between Ni(II) and Cr(VI) has been investigated. A graphical method is presented which allows for the calculation of thermodynamic equilibrium constants. At pHs between 7.2 and 7.7, the mixed precipitate  $\text{NiCrO}_4 \cdot 3\text{Ni}(\text{OH})_2$  is the major species in the solid state. Its thermodynamic solubility constant is reported [9].

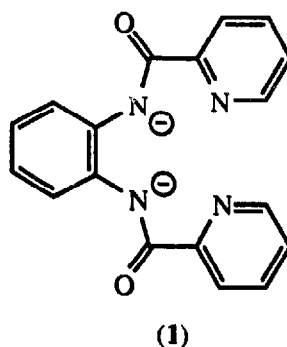
The compound  $(\text{HBpz}^*_3)\text{Cr}(\text{N}^t\text{Bu})_2\text{Cl}$  was reported. The complex has a pseudo-octahedral structure. The imido ligands are chemically equivalent from NMR spectroscopy. The IR spectrum is inconsistent with an uncoordinated pyrazolyl ligand [10].

## 9.2 CHROMIUM(V)

The reaction of potassium tris(2,3-quinoxalinedithiolato)chromium(V) with *o*-, *m*-, and *p*-phenylenediamine was examined by ESR spectroscopy. The *ortho* analogue displaces the ligands to form the corresponding tris(*o*-phenylenediamine) complex. One equivalent of the *para* analogue coordinates to the Cr in a monodentate fashion in the equatorial plane. The *meta* analogue does not react. The tris-chelates of Cr(V) have trigonally distorted octahedral structures [11].

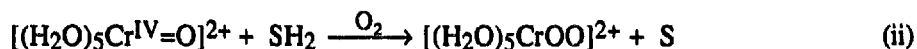
Chromium(III) salen and salpn complexes are oxidized by Ce(IV) to the Cr(V) Schiff base products. The iodosyl benzene oxidation of [Cr(Schiff base)(H<sub>2</sub>O)<sub>2</sub>]<sup>+</sup> produces a stable Cr(V) intermediate [12].

ESR and UV/VIS spectral measurements have been performed for the square pyramidal nitrido complex, CrN(L), where L is the dianion of *N,N'*-bis(pyridine-2-carbonyl)-*o*-phenylenediamine, (1). The Cr≡N bond displays a high degree of covalent character as a result of a strong dπ-pπ interaction [13].



## 9.3 CHROMIUM(IV)

The kinetics for the oxidation of a series of 1,2-diols by pentaqua(oxo)chromium(IV), CrO<sup>2+</sup>, were examined. The reaction proceeds according to equation (ii). The formation of the superoxochromium(III) ion suggests that a one-step two-electron reduction process occurs. A hydride abstraction mechanism is proposed for the oxidation of primary and secondary diols by CrO<sup>2+</sup> [14].



Vibrational analyses of a number of Cr(IV) fluorides were performed. Solid CrF<sub>4</sub> exhibits bands indicative of a polymeric structure with six-coordinate chromium and two terminal and four bridging fluorine atoms. There appear to be no infrared-Raman coincidences, suggesting an inversion centre exists. Because of the distortion of the octahedron, six stretching bands are expected and found for XeF<sub>2</sub>·CrF<sub>4</sub>. The infrared and Raman spectra of XeF<sub>5</sub><sup>+</sup>CrF<sub>5</sub><sup>−</sup> are consistent with the presence of a distorted fluorochromate(IV) octahedron. The spectra suggest the presence of polymeric fluorometallate anions for (XeF<sub>5</sub><sup>+</sup>CrF<sub>5</sub><sup>−</sup>)<sub>4</sub>·XeF<sub>4</sub> [15].

The cation  $[\text{Cr}(\text{Me}_4[14]\text{tetraene})(\text{H}_2\text{O})_2]^{4+}$  has been generated electrochemically from the corresponding Cr(III) cation. Although cyclic voltammetry reveals a quasi-reversible Cr(III/IV) wave for this macrocyclic complex, the salen and salpn complexes exhibit no redox wave in the region examined. The Cr(III) salen and salpn complexes are oxidized by Ce(IV) to the Cr(V) Schiff base products via a long-lived Cr(IV) intermediate. Visible and ESR spectral results are reported [16].

## 9.4 CHROMIUM(III)

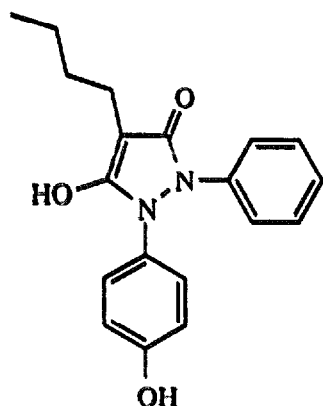
### 9.4.1 Complexes with monodentate ligands

Starting from *fac*- $[\text{Cr}(\text{NH}_3)_3(\text{TfO})_3]$ , the complexes *fac*- $[\text{Cr}(\text{NH}_3)_3(\text{L})_3]^{3+}$  ( $\text{L} = \text{CH}_3\text{CN}$ , dmso, and dmf) and *fac*- $[\text{Cr}(\text{NH}_3)_3(\text{X})_3]$  ( $\text{X} = \text{HCO}_2^-$ ,  $\text{NCS}^-$ ,  $\text{Br}^-$ ,  $\text{N}_3^-$ ) were prepared. The configurations were assigned based on the characteristic narrow transition observed at  $g = 2$  in the ESR spectra. The  $\text{NCS}^-$  ligand is *N*-bonded and dmso and dmf are *O*-bonded based on a comparison of the optical absorption spectra with similar *fac* compounds [17].

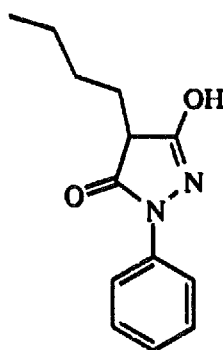
A series of  $[\text{Cr}(\text{III})\text{X}_3(\text{py})_3]$  complexes with  $\text{X} = \text{F}$ ,  $\text{Cl}$ ,  $\text{Br}$ , and  $\text{NCS}$  were synthesized. The geometries were assigned based on  $^2\text{H}$  NMR spectroscopy of the  $\text{py-d}_5$  analogues and on the UV-VIS spectra. For  $\text{X} = \text{NCS}$ ,  $\text{F}$  and  $\text{Br}$ , the complexes were assigned the *mer* geometry. However, for  $\text{X} = \text{Cl}$ , spectroscopic evidence supports the *fac* geometry [18].

The structure of  $[\text{Cr}(\text{NH}_3)_5\text{NCO}](\text{NO}_3)_2$  was determined by X-ray crystallography and an AOM analysis was performed. The cation has  $C_{4v}$  symmetry and the linear NCO group is *N*-bonded. Hydrogen-bonding interactions are observed between the nitrate anion and the axial ammonia ligand. The bonding properties of the  $\text{NCO}^-$  ligand are compared to  $\text{NCS}^-$  [19].

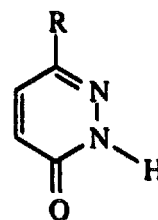
The complexes  $\text{Cr}(\text{L})_3(\text{OH})_3$  where  $\text{L} =$  oxyphenbutazone (2) [20] and monophenbutazone (3) have been synthesized [21]. Each ligand exists as keto-enol tautomers. Figures (2) and (3) represent the keto forms. Based on IR spectroscopic data, coordination is via the non-tautomeric carbonyl group of the keto form.



(2)



(3)



(4)

The potassium salts of the complex anions  $[\text{CrL}_2(\text{NCS})_4]^-$ , where L is the *p*-chlorophenyl-, *p*-bromophenyl-, or *p*-tolyl- derivative of pyridazone were synthesized from  $\text{K}_3[\text{Cr}(\text{NCS})_6]$ . The linkages of the ligands were assigned based on IR spectroscopy. The  $\text{NCS}^-$  ligands are *N*-bonded. Coordination of the pyridazone is via the amine nitrogen in the keto tautomer, (4) [22].

The syntheses of the compounds  $\text{A}_2\text{CrCl}_5\cdot\text{H}_2\text{O}$  (A = Cs, Rb) from  $\text{CrCl}_3\cdot 6\text{H}_2\text{O}$ , HCl, and the corresponding alkali metal acetate in acetic acid were described [23]. Dehydration of solutions of the salts with acetyl chloride was used to produce  $\text{A}_3\text{CrCl}_6$  and  $\text{A}_3\text{Cr}_2\text{Cl}_9$ . X-ray powder diffraction studies were performed from which the lattice parameters of the compounds were determined.

Water exchange in  $[\text{Cr}(\text{MeNH}_2)_5\text{H}_2\text{O}]^{3+}$  was studied as a function of temperature and pressure [24].  $^{17}\text{O}$  NMR spectroscopy was used to monitor the process. Rate constants and activation parameters were evaluated:  $k_{\text{ex}}^{298} = 4.1 \times 10^{-6} \text{ s}^{-1}$ ,  $\Delta H^\ddagger = 98.5 \text{ kJ mol}^{-1}$ ,  $\Delta S^\ddagger = -17.5 \text{ J K}^{-1} \text{ mol}^{-1}$ , and  $\Delta V^\ddagger = -3.8 \text{ cm}^3 \text{ mol}^{-1}$ . Comparison with the Co(III) and Rh(III) aquapentakis(methylamine) cations and the analogous aquapentaammine complexes suggests that steric demands of the inert complex skeleton increase the dissociative character of the interchange intimate mechanism.

Linkage isomerism has been demonstrated in the adducts formed between  $\text{Hg}^{2+}$  and  $[\text{Cr}(\text{NH}_3)_5\text{CN}]^{2+}$ . Two adducts were isolated with the formulas  $\{[\text{Cr}(\text{NH}_3)_5(\text{NC})]_4\text{Hg}\}(\text{ClO}_4)_{10}$  and  $\{[\text{Cr}(\text{NH}_3)_5(\text{NC})]_2\text{Hg}\}(\text{ClO}_4)_6$ . Rates of formation to yield the 2:1 adduct were determined by measuring the loss of phosphorescence of  $[\text{Cr}(\text{NH}_3)_5\text{CN}]^{2+}$ . The production of the adduct follows a two-term rate law. Each of the parallel paths involves an initial association equilibrium followed by linkage isomerization. The adducts undergo aquation to yield  $[\text{Cr}(\text{NH}_3)_5(\text{H}_2\text{O})]^{3+}$  and  $\text{Hg}(\text{CN})^+$  [25].

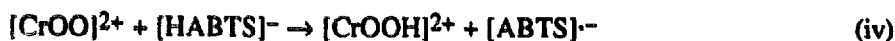
The complexes  $[\text{Cr}(\text{NH}_3)_6]\text{X}_3$ ,  $[\text{Cr}(\text{NH}_3)_5\text{Cl}]\text{Y}_2$ , and  $[\text{Cr}(\text{NH}_3)_5(\text{H}_2\text{O})]\text{Z}_3$  ( $\text{X}^- = \text{Br}^-$  or  $\text{NO}_3^-$ ,  $\text{Y} = \text{Cl}^-$  or  $\text{ClO}_4^-$ , and  $\text{Z} = \text{ClO}_4^-$  and  $\text{OTf}^-$ ) were studied using NI-FT-Raman spectroscopy. The symmetries and general valence force constants for the metal-ligand bonds were considered.  $[\text{Cr}(\text{NH}_3)_6]\text{Br}_3$  exhibits a splitting of the  $\text{A}_{1g}$  Cr-N stretching mode, perhaps a result of hydrogen bonding. For  $[\text{Cr}(\text{NH}_3)_5(\text{H}_2\text{O})]^{3+}$ , the Cr-N stretching frequency is about  $40 \text{ cm}^{-1}$  lower than the Cr-O frequency, indicating that the force constant of the Cr-O bond is larger than that of the Cr-N bond. Comparison of the stretching force constants for the examined complexes suggest that the nature of the hetero ligand has a large effect on the metal- $\text{NH}_3$  stretching vibration for the *trans*- $\text{NH}_3$  but a small effect on the *cis*- $\text{NH}_3$ . Results are compared to corresponding Co(III) complexes [26].

The homolysis of the superoxopentaaquachromium(III) ion has been investigated.  $[(\text{H}_2\text{O})_5\text{CrOO}]^{2+}$  was reacted with  $[\text{Ru}(\text{bpy})_3]^{3+}$ ,  $[\text{Fe}(\text{phen})_3]^{3+}$ , and  $[\text{Ru}(5,6\text{-Me}_2\text{phen})_3]^{3+}$  to give  $[\text{Cr}(\text{H}_2\text{O})_6]^{3+}$  and  $\text{O}_2$ . The observed rate constants are in agreement with those calculated using Marcus theory. The suggested mechanism involves a rate-determining oxidation to give  $[(\text{H}_2\text{O})_5\text{CrOO}]^{3+}$  followed by an extremely rapid homolysis to give the final products. The one-electron oxidation of  $[(\text{H}_2\text{O})_5\text{CrOO}]^{2+}$  increases the homolysis rate of the Cr-O bond by at least ten orders of magnitude [27].

The aquated complexes of Cr(III) and superoxide and hydroperoxide have also been studied using electrochemical techniques. The reduction of proceeds in two steps. The formal potential for the  $(\text{H}_2\text{O})_5\text{CrOO}^{2+}/(\text{H}_2\text{O})_5\text{CrOOH}^{2+}$  couple was found to be 0.97V vs NHE. The first product,  $(\text{H}_2\text{O})_5\text{CrOOH}^{2+}$  undergoes a further two-electron reduction to give  $\text{Cr}^{3+}$  and water at  $-0.07$  V vs NHE. However, the metastable hydroperoxide complex undergoes a spontaneous decomposition as shown in equation (iii). An analysis of the electrochemical data was used to deduce that the affinity of  $\text{Cr}^{3+}$  for  $\text{O}_2$  is extremely small [28].



Using the reaction shown in equation (iv), where  $\text{ABTS}^{2-}$  is 2,2'-azinobis(3-ethylbenzothiazoline-6-sulfonate), an examination of the way in which metal complexes facilitate the step-wise process of oxygen reduction to water was performed. The complete breakdown of the process into single-electron steps was allowed using data for  $\text{CrOO}^{2+}$ ,  $\text{CrOOH}^{2+}$ , and  $\text{Cr=O}^{2+}$ . The complete Latimer diagram for the four-electron reduction of oxygen to water with and without assistance from chromium was devised. Although  $\text{HO}^\cdot$  and  $\text{CrO}^{2+}$  sometimes react in similar fashions,  $\text{CrO}^{2+}$  has a propensity to undergo a two-electron conversion to  $\text{Cr}^{2+}$  when it reacts with an O atom acceptor, thereby having the advantage of a lower free energy pathway not available to  $\text{HO}^\cdot$ . Other reactions discussed include the reaction of  $\text{Fe}^{2+}$  with  $\text{CrO}^{2+}$  in which an oxo-bridged intermediate is proposed [29].



XPS and UPS have been used to probe the valence band of  $\text{CrCl}_3$ . The  $3d$  state of the chromium and the  $3p$  state of the chlorine compose the valence band. The compound is classified as a Mott-Hubbard insulator. The band gap corresponds to intercationic  $d-d$  transitions. The  $d-d$  Coulomb correlation energy is 2.8–3.0 eV [30].

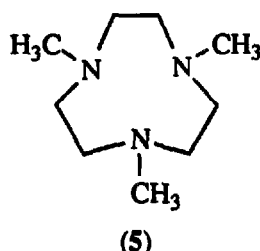
#### 9.4.2 Complexes with didentate ligands

##### 9.4.2.1 Oxygen donor ligand systems

The crystal structure of  $\text{NaMg}[\text{Cr}(\text{ox})_3] \cdot 10\text{H}_2\text{O}$  was reported. The average Cr–O bond distance is 197.4 pm. The average O–Cr–O angle for the five-membered rings is  $82.7^\circ$ . The average O–Cr–O angle between ligands is  $92.4^\circ$ . The largest deviation in the coordination sphere from  $180^\circ$  for *trans* O–Cr–O is  $16^\circ$ . The  $\text{Mg}^{2+}$  ion exists in two different environments, thereby creating two different ligand field environments for the complex anion [31]. The structure of  $\text{Li}_3[\text{Cr}(\text{ox})_3] \cdot 6\text{H}_2\text{O}$  was also determined [32]. The average Cr–O bond length in this salt is 197.9 pm and the average O–Cr–O angle in a chelate ring is  $82.3^\circ$ . The  $\text{Li}^+$  ions are coordinated by the oxygen atoms of both water and oxalato ligands. The three lithium ions are in distorted octahedral, square-pyramidal, and tetrahedral environments.

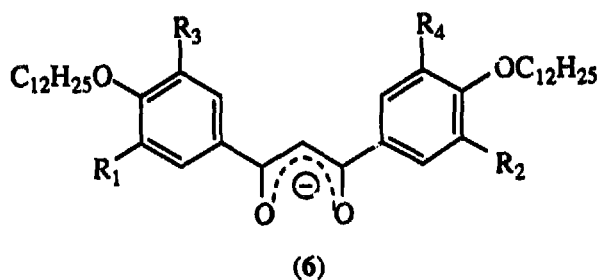
EXAFS spectra were obtained for  $K_3[Cr(ox)_3] \cdot 3H_2O$  in the solid state and in  $H_2O$ ,  $MeOH$ ,  $EtOH$ , and  $dmf$ . The calculated Cr–O distance increases with decreasing solvent acceptor number, ranging from 197.0 pm in  $H_2O$  to 197.3 pm in  $dmf$ . The authors suggest that solvatochromic effects observed for this complex are partly due to solvent effects on the Cr–O bond distance [33].

A remarkable solid-state transformation of  $[(CrL(acac))_2(\mu-H_3O_2)][PF_6]_3$ , where L is (5), to  $[CrL(acac)F]PF_6$  and  $[CrL(acac)(O_2PF_2)]PF_6$  with the simultaneous loss of three equivalents of HF is described. The process was monitored via thermal gravimetric analysis. The corresponding Co(III) complex does not undergo the transformation, even though the *bis*-Co(III) and *bis*-Cr(III)  $\mu-H_3O_2$  complexes are isostructural. The products may be selectively isolated from a solution  $[(CrL(acac))_2(\mu-H_3O_2)][PF_6]_3$  by adjusting the pH. A mechanism for the process is proposed. The structures of the complexes  $[CrL(acac)(OH_2)][ClO_4]_2$ ,  $[CrL(acac)F]PF_6$  and  $[CrL(acac)(O_2PF_2)]PF_6$  are described. Each contains a  $Cr^{III}L(acac)$  unit with L facially coordinated. The  $acac^-$  ligand is unremarkable in each case. The  $O_2PF_2^-$  ligand is monodentate and bonds via one of the oxygen atoms [34].



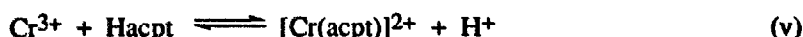
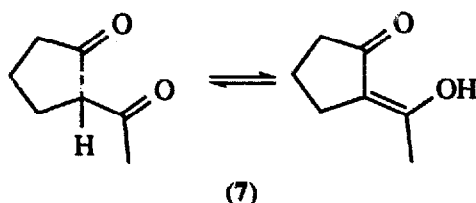
A method is described for the synthesis of Cr(III)  $\beta$ -diketonates from boron difluoride  $\beta$ -diketonates and  $CrCl_3 \cdot 6H_2O$  in  $dmf$ . The complexes  $Cr(MeCOCHCOR)_3$ , where  $R = Me, Ph, p-CH_3C_6H_4$ , and  $t-Bu$ , were synthesized. UV-VIS spectral data are reported [35].

A series of *tris*  $\beta$ -diketonate complexes of Cr(III) having the formula  $CrL_3$ , where L is the ligand (6) with  $R_1 = R_2 = OC_{12}H_{25}$ ,  $R_3 = R_4 = H$ ;  $R_1 = R_2 = R_3 = OC_{12}H_{25}$ ,  $R_4 = H$ ; and  $R_1 = R_2 = R_3 = R_4 = OC_{12}H_{25}$  have been synthesized. Along with the Fe(III) and Co(III) complexes, they display mesomorphism. X-ray diffraction studies have been used to explore the phase transitions of these complexes [36].



The reaction of  $Cr^{3+}$  with Hacpt, (7), was monitored spectrophotometrically under conditions in which only a 1:1 complex forms. The equilibrium constant is 89.3 for reaction (v). Formation of the complex proceeds by two pathways. Activation parameters are tabulated. The

pathway involving  $\text{Cr}(\text{OH})^{2+}$  is faster than that involving  $\text{Cr}^{3+}$  ( $k = 5.48 \times 10^{-2} \text{ mol}^{-1} \text{ s}^{-1}$  and  $2.41 \times 10^{-2} \text{ mol}^{-1} \text{ s}^{-1}$ , respectively) for reaction with the enol form of the ligand [37].

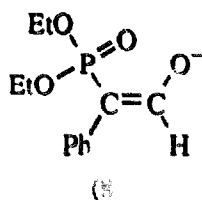


The preparation of bis(aminoacidato)(aminoacidato-*N*)(dmso) complexes of Cr(III),  $\text{Cr}(\text{AA})_2(\text{AA-}N)(\text{dmso})$ , where AA = L-valine, L-isoleucine, and L-leucine, was described. All complexes are shown to have the facial configuration as were the corresponding  $\text{Cr}(\text{AA})_3$  complexes. The complexes are stable and isomerize readily from the  $\Lambda$ -isomer to the  $\Delta$ -isomer in non-aqueous solvents. Under certain conditions, the conversion from  $\text{Cr}(\text{AA})_2(\text{AA-}N)(\text{L})$  to  $\text{Cr}(\text{AA})_3$  occurs [38].

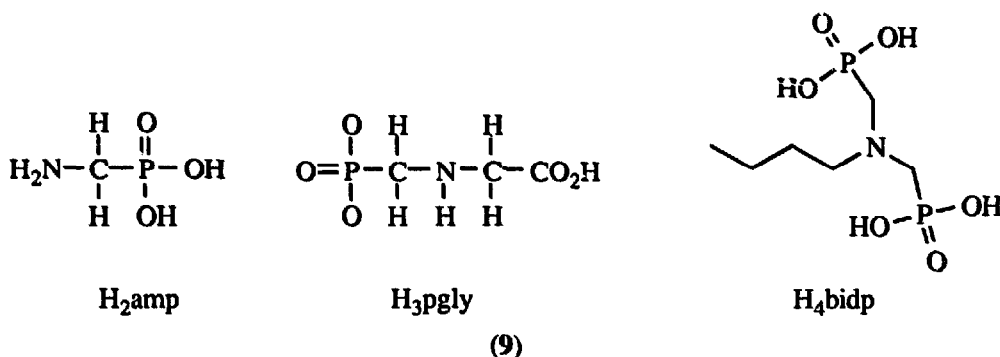
Polyvinyl alcohol complexes of Cr(III) were prepared. The properties were compared with those of Cu(II) complexes. The composition of the resulting complexes varied from 10 to 40%  $\text{Cr}(\text{NO}_3)_3$  by mass. As the concentration of Cr(III) increases, so does the volumetric heat capacity. The value also increases with temperature. The thermal diffusivity and thermal conductivity become larger with temperature and concentration of metal salt, too, and are larger than those of pure polyvinyl alcohol. The thermal conductivity of the corresponding Cu(II) complexes were larger than those of Cr(III) [39].

The preparation and characterization of a Cr(III) secondary cellulose acetate complex was described. The green complex was characterized by elemental analysis, magnetic susceptibility, and IR, NMR, and UV-VIS spectroscopic studies. A structure is proposed in which the Cr(III) is in an octahedral environment with axial water ligands. Uncoordinated acetate is present [40]. Cr(III) complexation with carboxymethyl cellulose (CMC) was also examined. Measurements were obtained in the solid state and in solution. CMC coordinates to chromium to give  $\text{Cr}(\text{CMC})_2(\text{H}_2\text{O})_2$ . Again, the water ligands occupy axial sites [41].

The synthesis of tris(2-diethoxyphosphonyl-2-phenylethen-1-olato)chromium(III),  $\text{Cr}(\text{L})_3$ , was described. The ligand is shown in (8); the product is a green oil. The iron(III) complex was isolated as a crystalline solid and subjected to X-ray analysis. The structure of  $\text{Cr}(\text{L})_3$  is inferred from the iron complex. The electronic spectrum is consistent with an octahedral complex [42].







The syntheses of a series of aminophosphonate Cr(III) complexes were reported. Molecular mechanics, semi-empirical, and *ab initio* calculations were performed. The aminophosphonates examined coordinate in a didentate fashion and their abbreviations are shown in figure (9). The stretching modes of the PO<sub>3</sub> group were used to infer that coordination occurred via the phosphonate moiety. IR spectroscopy was used to infer carboxylate coordination in the H<sub>3</sub>pgly derivative. Electronic spectroscopy was used to assign the coordination geometry. For [Cr(Hamp)<sub>2</sub>(H<sub>2</sub>O)]Cl, calculations show that the two water molecules are *trans*. The *cis* isomer is 62 kJ mol<sup>-1</sup> higher in energy based on MMX force field calculations. In K[Cr(H<sub>2</sub>bipd)<sub>2</sub>(H<sub>2</sub>O)<sub>2</sub>], <sup>31</sup>P NMR spectroscopy was used to deduce the equivalence of the phosphorus atoms, which suggests that the H<sub>2</sub>bipd<sup>2-</sup> ligand coordinates using one oxygen atom from each of the phosphonates. Molecular modelling predicts that the *trans* isomer is 92 kJ mol<sup>-1</sup> lower in energy than the *cis* H<sub>2</sub>O structure and that the coordinated water is stabilized by H-bonding interactions. The chromatographic behaviour of K[Cr(Hpily)<sub>2</sub>(H<sub>2</sub>O)<sub>2</sub>] was used to deduce its structure. The relative elution order suggested that it was more polar than the comparison complexes and so a *cis* H<sub>2</sub>O structure was postulated. Hpily<sup>2-</sup> coordinates in a didentate fashion via the carboxy group and one oxygen of the phosphonate [43].

#### 9.4.2.2 Nitrogen donor ligand systems

The structures of [Cr(en)<sub>3</sub>]<sub>3</sub>[FeCl<sub>6</sub>]Cl<sub>6</sub>·H<sub>2</sub>O and [Cr(en)<sub>3</sub>]<sub>3</sub>[FeCl<sub>4</sub>]Cl<sub>2</sub>·9H<sub>2</sub>O were reported. Magnetic data for [Cr(en)<sub>3</sub>]<sub>3</sub>[FeCl<sub>6</sub>]Cl<sub>6</sub>·H<sub>2</sub>O, [Cr(en)<sub>3</sub>]<sub>3</sub>[FeCl<sub>6</sub>] and [Cr(en)<sub>3</sub>]<sub>3</sub>[InCl<sub>6</sub>] were also obtained. For [Cr(en)<sub>3</sub>]<sub>3</sub>[FeCl<sub>6</sub>]Cl<sub>6</sub>·H<sub>2</sub>O, X-ray crystallography shows that discrete [Cr(en)<sub>3</sub>]<sup>3+</sup>, [FeCl<sub>6</sub>]<sup>3-</sup>, and Cl<sup>-</sup> ions exist. The average Cr-N bond distance is 207 pm. The average N-Cr-N angle in the five-membered rings is 82.6°. An extensive H-bonding network exists. The [Cr(en)<sub>3</sub>]<sup>3+</sup> cations are linked to the complex anions and the Cl<sup>-</sup> anions by N-H...Cl interactions and the water molecules are related to the Cl<sup>-</sup> anions via O-H...Cl interactions. Discrete complex ions, Cl<sup>-</sup> anions, and water molecules exist in the structure of [Cr(en)<sub>3</sub>]<sub>3</sub>[FeCl<sub>4</sub>]Cl<sub>2</sub>·9H<sub>2</sub>O. The Cr atom sits on a three-fold axis. The average of the two independent Cr-N bond distances is 212 pm. The N-Cr-N angle in the independent five-membered ring is 82.5°. Although an extensive H-bonding network exists in this salt, no N-H...Cl bonds connect the complex cations to the complex anions. However, neighbouring [Cr(en)<sub>3</sub>]<sup>3+</sup> ions are related by N...Cl hydrogen bonds and

neighbouring  $[\text{FeCl}_4]^-$  ions are related by  $\text{O}\cdots\text{Cl}$  hydrogen bonds.  $[\text{Cr}(\text{en})_3][\text{FeCl}_6]\text{Cl}_6\cdot\text{H}_2\text{O}$  displays magnetic characteristics consistent with a ferromagnetic interaction between the octahedral high-spin  $\text{Fe}(\text{III})$  and the  $\text{Cr}(\text{III})$  ions. The magnetic behaviour of  $[\text{Cr}(\text{en})_3][\text{FeCl}_6]$  is quite different and is consistent with antiferromagnetic interactions between the metal centers.  $[\text{Cr}(\text{en})_3][\text{InCl}_6]$  exhibits magnetic character expected of paramagnetic material ( $S = 3/2$ ). Arguments are made for the involvement of H-bonding in the superexchange pathways between magnetic centers [44].

The aquation reaction of  $\text{cis}-[\text{Cr}(\text{en})_2(\text{H}_2\text{O})\text{Br}]^{2+}$  was examined in mixed-solvents consisting of water and  $\text{MeOH}$ ,  $\text{EtOH}$ ,  $i\text{-PrOH}$ , or  $t\text{-BuOH}$ . A comparison of the kinetic data and activation parameters is made with those in water. The addition of non-aqueous cosolvent leads to a destabilization of both the complex ion and the transition state, as a decrease in solvent polarity disfavours breaking the  $\text{Cr}-\text{Br}$  bond. The process is described as solvent-modified dissociative interchange,  $\text{I}_\text{d}$  [45].

The angular overlap model parameters are derived for  $\text{Cr}(\text{III})$  complexes with  $D_{2h}$  and  $C_{2v}$  symmetry. These are based on a method developed for the analysis of d-d transition energies. The method allows one to take into account deviations from tetragonal symmetry for complexes of the type  $\text{trans}-[\text{MXY}(\text{AA})_2]$  in which the bite angle may deviate significantly from  $90^\circ$ . As a demonstration of its utility, successful application is made to the complexes  $\text{trans}-[\text{CrF}_2(\text{en})_2]^+$  and  $\text{trans}-[\text{CrF}(\text{H}_2\text{O})(\text{en})_2]^+$  [46].

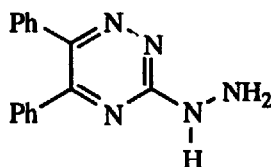
$\text{Tris}[(\pm)\text{-trans-1,2-cyclohexanediamine}]\text{chromium(III) chloride}$ ,  $[\text{Cr}(\text{chxn})_3]^{3+}$ , was subjected to spectral analysis including low temperature luminescence and excitation spectroscopies and UV-VIS and IR spectroscopies at room temperature. The relationship between geometry and the sharp-line electronic transitions was examined. The amine exhibits strong  $\sigma$ -donor characteristics. The didentate ligand bite angle and twist angles were used to specify the geometry of the complex. The eight components of the  $^4\text{A}_{2g} \rightarrow ^2\text{E}_g$ ,  $^2\text{T}_{1g}$ , and  $^2\text{T}_{2g}$  transitions are especially sensitive to the geometry of the ligand [47].

The synthesis and photoproperties of  $\text{Na}[\text{Cr}(\text{tn})(\text{CN})_4]$ , where  $\text{tn} = 1,3\text{-diaminopropane}$ , have been reported. This complex exhibits properties which make it a candidate for use as a quencher. A comparison of the  $[\text{Cr}(\text{tn})_3]^{3+}$  quenching ability of  $[\text{Cr}(\text{tn})(\text{CN})_4]^-$  and hydroxide was made.  $[\text{Cr}(\text{tn})(\text{CN})_4]^-$  compares favourably and has the advantage that the acceptable pH range is 2–10. Although it does undergo some light absorption, acid-catalysed thermal aquation, and photodecomposition, linear Stern-Volmer quenching plots were obtained. In the examination of the photoproducts for the fully quenched photoaquation of  $[\text{Cr}(\text{tn})_3]^{3+}$ , a higher yield of the *cis* isomer of  $[\text{Cr}(\text{tn})_2(\text{tnH})(\text{H}_2\text{O})]^{4+}$  than the *trans*-isomer was obtained when compared to the unquenched reaction. The data are consistent with 35% *cis*-product from the reaction via the doublet and 47% *cis* from the quartet [48]. Contrary to an earlier report [49], no increase in the percent *cis* isomer on irradiation in the red edge of the quartet band was observed. The discrepancy is blamed on concurrent thermal photolysis during the earlier study.

The displacement of water ligands from the complex  $\text{cis}-[\text{Cr}(\text{biguanide})_2(\text{H}_2\text{O})_2]^{3+}$  by pyridine-2-aldoxime,  $\text{Hpa}$ , was studied. The aquation rate constant is pH dependent. The process appears to follow an  $\text{I}_\text{a}$  mechanism in which an outer-sphere complex between the cation and the  $\text{Hpa}$  is followed by simultaneous coordination of  $\text{pa}^-$  and loss of  $\text{H}_3\text{O}^+$  and  $\text{H}_2\text{O}$ .  $\Delta\text{H}^\ddagger$  decreases

with a decrease in the dielectric constant of the reaction medium and  $\Delta S^\ddagger$  becomes more negative [50]

The complex  $[\text{Cr}(\text{L})_2\text{Cl}]\text{Cl}$ , where  $\text{L} = 3\text{-hydrazino-5,6-diphenyl-1,2,4-triazine}$ , (**10**), has been synthesized and characterized. The complex is electrolytic in nature and conductance measurements indicate a 1:1 ratio of cation to anion. The ligand field parameters are reported. IR spectroscopy was used to assign the linkage as via the amine nitrogen and N-2 rather than N-4 [51].



(10)

The redox reactions of  $[\text{Cr}(\text{NN})_3]^{3+}$  complexes, where  $\text{NN} = \text{bpy}$ , 4,4'- $\text{Me}_2\text{bpy}$  or phen, with *meta* and *para*-substituted phenylthioacetic acids,  $\text{RPhSCH}_2\text{CO}_2\text{H}$ , were studied with luminescence quenching techniques. In acetonitrile, the quenching rate is found to be accelerated when the phenyl ring is substituted with electron releasing groups and follows the order  $[\text{Cr}(\text{bpy})_3]^{3+} > [\text{Cr}(\text{dmbpy})_3]^{3+} > [\text{Cr}(\text{phen})_3]^{3+}$ . In water, the rates are two to three orders of magnitude faster. The explanation offered is that the electron donor is the carboxyl group in water whereas the sulfur is the electron donor in acetonitrile [52].

Spectral hole burning experiments in the presence of a magnetic field have been performed for  $[\text{Cr}(\text{bpy})_3]^{3+}$  in glycerol. Better agreement with the data is obtained when a distribution of fields with lower than trigonal symmetry is used in the fitting procedure. Explanations include the arrangement of solvent molecules, ion pairing, or a tipping of the bpy ligands [53].

The synthesis of  $[(\text{bpy})_2\text{Cr}\{\text{CNRu}(\text{NH}_3)_5\}_2](\text{PF}_6)_5$  and metal-to-metal charge transfer,  $\text{MM}'\text{CT}$ , spectroscopy studies for this and other complexes of the type  $\text{LM}\{\text{CNRu}(\text{NH}_3)_5\}$  are reported. The  $\text{Ru}(\text{III/II})$  couple is sensitive to the nature of  $\text{M}$  and  $\text{L}$ . For the  $\text{Cr}(\text{III})$  complex in acetonitrile,  $E_{1/2} = 0.295 \text{ V vs SCE}$ . Based on spectroscopic and electrochemical data,  $\text{MM}'\text{CT}$  stabilization energies are much smaller for complexes with a Co central metal than for Ru, Fe, and Cr metals. The effect of  $d\pi\text{-}d\sigma$  vs  $d\pi\text{-}d\pi$  interactions is discussed [54].

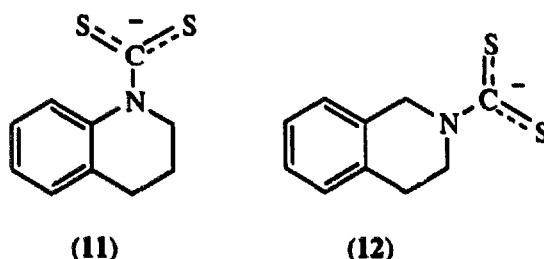
Flash and continuous photolysis studies of phenol in aqueous solutions were conducted using  $[\text{Cr}(\text{bpy})_3]^{3+}$  as a sensitizer. In the flash photolysis experiments, bleaching of the ground state was observed, but no evidence for  $[\text{Cr}(\text{bpy})_3]^{2+}$  was found, consistent with a very low cage escape yield for the electron transfer process. In the presence of air, 1,4-benzoquinone and  $[\text{Cr}(\text{bpy})_2(\text{H}_2\text{O})_2]^{3+}$  were produced with a quantum yield that depends on pH ( $\Phi = 1.5 \times 10^{-4}$  at pH 2) [55].

#### 9.4.2.3 Sulfur donor ligand systems

A series of dimetallic assemblies with dithiooxalato, dto, bridges of the form  $[\text{NiPr}_4\{\text{MCr}(\text{dto})_3\}]_x$  ( $\text{M} = \text{Fe}(\text{II})$ ,  $\text{Co}(\text{II})$ ,  $\text{Ni}(\text{II})$ ,  $\text{Zn}(\text{II})$ ) were reported. The dto ligand coordinates

using the *S,S'*-mode to Cr(III) and the *O,O'*-mode to M(II). The magnetic properties were explored. The Zn analogue obeys the Curie law and the magnetic moment is practically independent of temperature in the range 5–300 K. The other complexes obey Curie-Weiss behaviour for 300 to 70 K, with the metals behaving as independent paramagnetic centers. However, below 70 K, the magnetic moment increases sharply. The Ni(II) complex displays more complicated low-temperature behaviour with two-steps occurring in the transition. The ferromagnetic phase-transition temperatures occur at 8, 16, and 23 K for the Fe(II), Co(II), and Ni(II) complexes, respectively. These values are compared with those of the corresponding oxalato bridged complexes [56].

The synthesis and spectroscopic characterization of complexes of Cr(III) with the dithiocarbamates of tetrahydroquinoline, (11), and tetrahydroisoquinoline, (12), were reported. The two complexes are non electrolytes in dmf and have the formula Cr(dtc)<sub>3</sub>. The UV-VIS spectra are consistent with a CrS<sub>6</sub> chromophore with a distorted octahedral structure. The EPR spectra exhibit one broad signal [57].



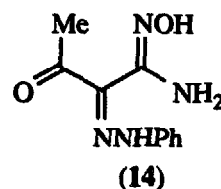
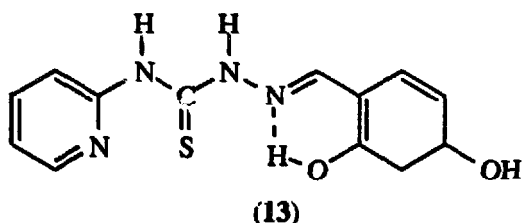
#### 9.4.2.4 Mixed donor ligand systems

The thermal isomerization of a series of *fac*-tris(amino acid)Cr(III) complexes has been examined. The complexes have the formula Cr(AA)<sub>3</sub>, where AA represents conjugate bases of the L-amino acids alanine (ala), norvaline (nval), norleucine (nleu), valine (val), leucine (leu), and isoleucine (ileu). In all cases examined, the products of the isomerization were *fac*. The results allow the classification of the AAs into two types based on the mixtures of diastereoisomers obtained after heating. For unbranched AAs such as ala, nval and nleu, thermal isomerization of  $\Lambda$ -complexes does not take place and  $\Delta$ -complexes undergo inversion to  $\Lambda$ . For the AAs val, ileu and leu, heating resulted in isomerization of both the  $\Lambda$ - and  $\Delta$ -complexes to mixtures of diastereoisomers. The latter observation led to the successful synthesis of the heretofore unisolated *fac*- $\Delta$ -[Cr(AA)<sub>3</sub>] complexes with AA = val, ileu, and leu via the thermal isomerization of the corresponding *fac*- $\Lambda$ -complex [58].

The compound 4-(2-pyridyl)-1-(2,4-dihydroxybenzaldehyde)-3-thiosemicarbazone, H<sub>3</sub>pbt (13), coordinates with Cr(III) to form Cr(H<sub>2</sub>pbt)(H<sub>2</sub>O)Cl. The H<sub>2</sub>pbt<sup>−</sup> behaves as a uninegative didentate ligand employing the deprotonated *ortho* OH and CN groups [59].

The synthesis and characterization of [CrL<sub>2</sub>(H<sub>2</sub>O)<sub>2</sub>](OAc)<sub>2</sub>Cl·2H<sub>2</sub>O where L = 3-oxo-2-phenylhydrozone-1-carbamidoxime, (14), was reported. Didentate coordination is through the

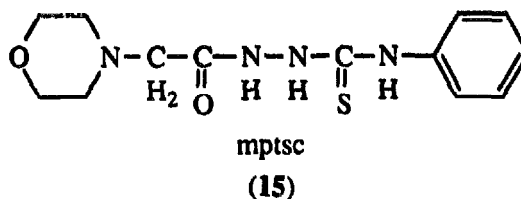
nitrogen of the hydrazone group and the carbonyl oxygen. The UV-VIS and IR spectra, magnetic susceptibility, and conductance measurements were used to characterize the complex [60].



The substitution of water ligands on *cis*-[Cr(BigH)<sub>2</sub>(H<sub>2</sub>O)<sub>2</sub>]<sup>3+</sup>, where BigH is biguanide, by glutamic acid, HL, has been examined in EtOH-H<sub>2</sub>O mixtures. The reaction product was identified as *cis*-[Cr(BigH)<sub>2</sub>L]<sup>2+</sup> by elemental analysis of the isolated product and by the construction of Job's plots. The activation parameters were determined. The enthalpy and entropy of activation decrease with the increase in EtOH concentration in the reaction medium. The data suggest an I<sub>a</sub> mechanism for anation in which the complex forms an outer-sphere association complex with HL followed by simultaneous Cr-OH<sub>2</sub> bond rupture and formation of the new Cr-L bonds [61].

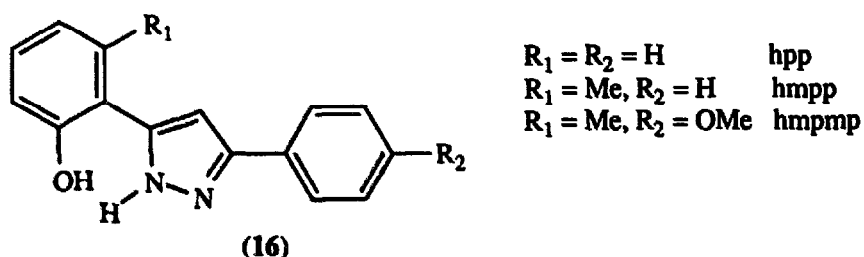
A salt of  $\Lambda$ -*cis*-[Cr(thiosemicarbazide)<sub>3</sub>]<sup>3+</sup> was synthesized and the UV-VIS and IR spectra obtained. No synthetic details were given. The corresponding Co(III) complex ion was obtained as the trihydrate chloride salt. The structure of this compound as determined by X-ray crystallography is reported. The Cr(III) complex ion displays an IR spectrum consistent with coordination through the sulfur and hydrozinic nitrogen atom. This coordination mode is exhibited by the Co(III) salt [62].

N<sup>1</sup>-(*N*-Morpholinoacetyl)-*N*<sup>4</sup>-phenyl thiosemicarbazide, (15), was reported to behave as a neutral didentate *N,S*-donor towards Cr(III) in the complex [Cr(mdbt)<sub>2</sub>Cl<sub>2</sub>](Cl·H<sub>2</sub>O). The complex was characterized by conductivity measurements (it is a 1:1 electrolyte in dmf), magnetic susceptibility determination, elemental analysis, UV-VIS and IR spectroscopies, and differential thermogravimetric analysis. The complex loses the water of hydration at about 120°C [63].



The complex formed by the reaction of 2-mercaptopnicotinic acid with [Cr(dmu)<sub>6</sub>](ClO<sub>4</sub>)<sub>3</sub>, where dmua is 1,3-dimethylurea, was studied by UV-VIS spectroscopy and polarographic techniques. A complex with a 3:1 ligand:metal ratio is formed, but only in the presence of two equivalents of base. If only the carboxylic acid group is deprotonated (one equivalent of base), no complexation occurs. The conditional formation constants were found to be 2.5 × 10<sup>14</sup> and 1.5 × 10<sup>14</sup> using polarographic and spectrophotometric analyses, respectively [64].

The coordination of the ligands (16) with Cr(III) has been studied. The  $pK$  values of the ligands follow the order  $hmpmp > hmpp > hpp$ . The stability constants are reported for the tris complexes of Cr(III), Fe(III), and Al(III). Binding follows the order  $Fe(III) > Cr(III) > Al(III)$  [65].



The interaction of Cr(III) complexes with DNA was examined. The salts  $K[Cr(asc)_2] \cdot 7H_2O$ ,  $K_2[Cr(OH)(asc)_2] \cdot 6H_2O$ ,  $K[Cr(asc)(cys)] \cdot 6H_2O$ , and  $K[Cr(asc)(gsh)] \cdot 6H_2O$ , where  $asc$  = ascorbate,  $cysH$  = cysteine, and  $gsh$  = glutathione, were used in this study. When dissolved in water, the UV absorption spectra of the complexes exhibit significant changes. The mixed-ligand complexes were more resistant towards reaction with water. When DNA was added to solutions of the complexes, shifts in the band positions and intensities were observed. Again, the changes with the mixed ligand systems were slightest. No interstrand cross-linking was observed with  $[Cr(asc)_2]^-$ ,  $[Cr(OH)(asc)_2]^{2-}$  or  $[Cr(asc)(gsh)]^-$ , but incubation with  $[Cr(asc)(cys)]^-$  resulted in the formation of about 6% double-stranded DNA [66].

#### 9.4.3 Complexes with polydentate ligands

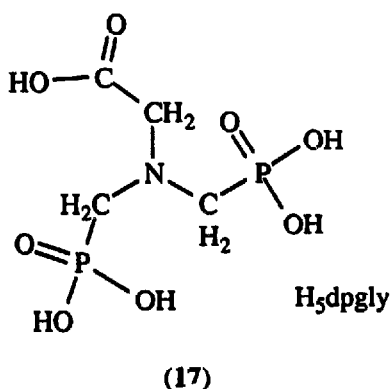
##### 9.4.3.1 Tridentate ligands

L-Lysine and L-glutamic acid complexes of Cr(III) were reported. The amino acid ligands are tridentate with meridional geometry. The meridional geometry is a result of the preference of the other ligand present, di(3-aminopropyl)amine, dapa, or glycolglycine, glygly, for meridional coordination. Molecular mechanics calculations were performed to establish the lowest energy geometries. The salts  $[Cr(dapa)(L-lys)]Cl_2 \cdot EtOH \cdot 0.5KCl$  and the potassium and barium salts of  $[Cr(glygly)(L-glu)]^-$  were examined [67].

The salts  $[CrCl(ampy)(dpt)](ClO_4)_2$  and  $[CrCl(ampy)(2,3-tri)]ZnCl_4 \cdot H_2O$  (ampy is 2-aminomethylpyridine, dpt is 1,5,9-triazanonane, and 2,3-tri is 1,4,8-triazaoctane) have been characterized by X-ray crystallography. Both the  $[CrCl(ampy)(dpt)]^{2+}$  and  $[CrCl(ampy)(2,3-tri)]^{2+}$  cations exhibit a *mer*  $N_3$  ligand with the secondary N proton *exo* form the chloro ligand. In the dpt complex, the py of the ampy is *trans* to the chloro ligand, but the amino group of the ampy ligand is *trans* to the chloro ligand in the 2,3-tri complex. The rates of acid hydrolysis,  $Hg^{2+}$ -assisted chloride release and base hydrolysis for these complexes were determined and compared to those of similar complexes [68].

The structure of the complex  $[\text{Cr}(\text{dapa})(\text{ida})]\text{ClO}_4 \cdot 2\text{H}_2\text{O}$ , where dapa is di(3-aminopropyl)amine and  $\text{H}_2\text{ida}$  is iminodiacetic acid, was determined. The ligands adopt a *fac* orientation with the two secondary nitrogen atoms *trans*. The average Cr-N bond distance is 208 pm and the Cr-O bond distances are 196 and 194 pm. The average intra-ligand N-Cr-N angle is  $92.3^\circ$  for dapa. Luminescence spectra were obtained at low temperature. The authors concluded that iminodiacetate carboxylate groups are moderately strong  $\sigma$ - and  $\pi$ -donors [69].

Two potassium salts of  $[\text{Cr}(\text{L-glu})_2]^-$ , where  $\text{gluH}_2$  is glutamic acid, were isolated and subjected to spectral analysis. In each, the glu is tridentate and coordinates *fac*. The N ligands are *cis* in both salts. However, in  $\text{K}[\text{Cr}(\text{L-glu})_2] \cdot 2\text{H}_2\text{O}$  the  $\text{O}_\alpha$  atoms are *trans* whereas the  $\text{O}_\gamma$  atoms are *trans* in  $\text{K}[\text{Cr}(\text{L-glu})_2] \cdot 1.5\text{MeOH} \cdot 2\text{H}_2\text{O}$ . The assignment is based on AOM model analysis of the absorption spectra of the complexes. Molecular modelling calculations predict that the *mer* configuration is lowest in energy [70].

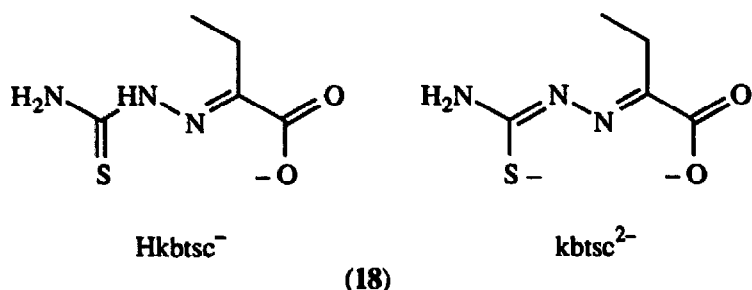


The syntheses of a series of aminophosphonate Cr(III) complexes in which tridentate coordination occurs were reported. Molecular mechanics, semi-empirical, and *ab initio* calculations were performed. The aminophosphonates examined that coordinate in a tridentate fashion are  $\text{H}_3\text{plgy}$  (9) and  $\text{H}_5\text{dpgly}$  (17). Of the six possible isomers for  $[\text{Cr}(\text{Hplgy})_2]^-$ , the five *fac* isomers have similar energies, but the *mer* isomer is the most stable based on modelling calculations. The complex  $\text{K}_3[\text{Cr}(\text{H}_2\text{dpgly})_2]$  has a molar conductance consistent with a 1:3 electrolyte. The UV-VIS spectral data are consistent with an  $\text{O}_6$  coordination geometry. The similarities of the free ligand N-H stretching frequencies with those in the complex support an absence of N coordination. According to molecular modelling calculations, the *fac* isomer with the *trans* carboxylate geometry is lower in energy than the *cis* isomer [71].

The interaction of ninhydrin with  $[\text{Cr}(\text{histidine})(\text{H}_2\text{O})_3]^{2+}$  was studied. The composition of the product was determined to be 1:1 using Job's method. The postulated mechanism involves coordination of the ninhydrin followed by interligand Schiff base condensation. As a result, the tridentate (N,O,N') histidine ligand is transformed into the tetradentate adduct (N,O,N',O) [72].

The crystal structure of  $\text{Cr}(\text{Hkbtsc})(\text{kbtsc})$ , where  $\text{H}_2\text{kbtsc}$  is 2-ketobutyric acid thiosemicarbazone, has been reported. The thiosemicarbazone is in two forms in this complex:  $\text{Hkbtsc}^-$  is the thione and  $\text{kbtsc}^{2-}$  is the thiol form (18). The chromium(III) is in a distorted octahedral environment with the tridentate ligands occupying meridional sites. The chelated ligand

adopts the *Z*-configuration. The intraligand bond distances support the assignment as thiol and thione. EPR and IR spectral and electrochemical data are reported. The complex exhibits three successive reduction peaks (−1.02, −1.12, and −1.59 V vs Ag/AgCl) which are irreversible. The first two are ligand-based. [73]



Using the electronic spectra of  $[\text{Cr}(\text{D-pen})_2]^-$  and  $[\text{Cr}(\text{D-pen})(\text{L-pen})]^-$ , where pen is penicillamine, an angular overlap model analysis was performed to determine the structures of the complex ions. Ligands are tridentate and display S,N,O coordination. Molecular models showed that the ligand can coordinate only *fac*. The D-complex was predicted to be the *trans*-S, *cis*-N, *cis*-O isomer and the D,L-complex to be the all *cis* isomer [74].

The synthesis and structure of  $[\text{CrCl}\{\text{N}(\text{CH}_2\text{CH}_2\text{PMe}_2)_2\}_2]$  was reported. The diphosphinoamido ligands employ two different coordination modes. One of the ligands is didentate (N,P) and the other is tridentate (P,N,P'). The amido nitrogens are *cis*. The tridentate ligand has *trans* phosphines. The didentate ligand Cr-N bond distance is about 2 pm shorter than the other. The geometry about the didentate amido nitrogen is described as tending toward planar, whereas the tridentate amido nitrogen is more pyramidal. This is ascribed to an increase in ligand to metal  $\pi$ - $\text{d}\pi$  interactions for the former compared to the latter [75].

#### 9.4.3.2 Tetradentate ligands

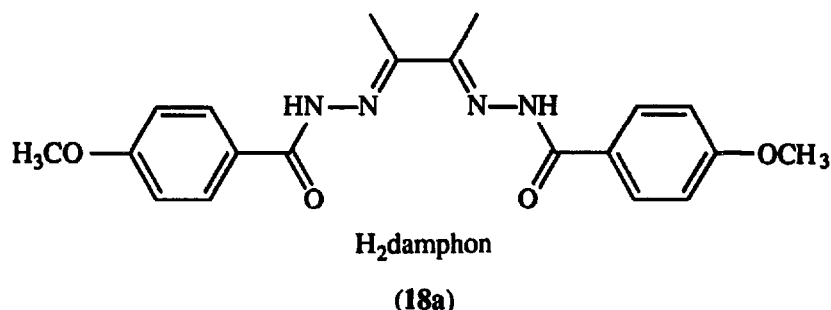
The photoaquation reaction of *trans*- $[\text{Cr}(\text{tet})(\text{CN})_2](\text{ClO}_4)$  was explored. The complex was irradiated at 436 nm. The photoproduct was identified as  $[\text{Cr}(\text{tetH})(\text{H}_2\text{O})(\text{CN})_2]^{2+}$ . From the fifteen isomers possible, all but the *mer* isomers with a protonated side-arm were eliminated. The arrangement of the  $\text{CN}^-$  ligand was assigned as *trans* based on UV-VIS spectroscopic data and the recoordination of the amine on the photoproduct [76]. The photochemistry was also examined by flash photolysis. The compound emits from the doublet state at 705 nm in water and dmso with an emission lifetime of 28  $\mu\text{s}$ . The photoreaction occurs within the same time frame, suggesting that the photoreaction occurs from the doublet state [77].

The crystal structure of  $[\text{Cr}(\text{acen})(\text{py})_2][\text{ZnCl}_3\text{py}]$  was determined. The py ligands occupy *trans* sites in the octahedral ligand array. There are two independent units in the asymmetric unit. The Cr-N(py) distances range from 207.9 to 212.4 pm. The disparity in the bond lengths is accounted for by a consideration of the orientation of the pyridine rings. The longer distances result



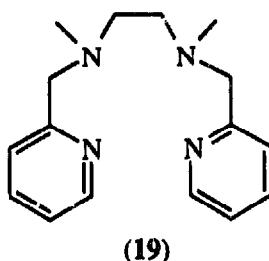
from steric interaction with the equatorial chelating ligand N and O atoms. Mean Cr–O and Cr–N(acen) bond lengths are 193.9 and 199.5 pm [78].

A series of Cr(III) complexes with the tetradentate ligand (18a) have been characterized. The Cr(III) is in an octahedral environment with additional ligands such as  $\text{NH}_3$ , py,  $\text{H}_2\text{O}$ , or  $\text{SCN}^-$ , or the didentate acac, salicylate, gly, or *N*-phenylsalicylaldimine ligands. Coordination of damphon is via *O,N,N',O'*-linkage with the  $\text{N}_2\text{O}_2$  moiety in the equatorial plane when the other ligands are monodentate. Coordination of a didentate linkage forces the damphon to adopt a nonplanar conformation [79].



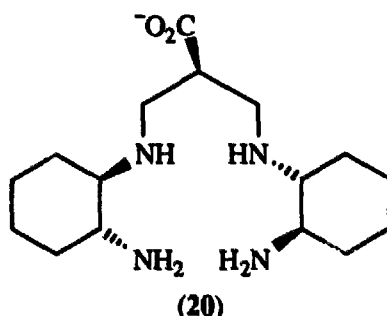
The protonation and substitution reactions of  $\text{NH}_4[\text{Cr}(\text{nta})(\text{H}_2\text{O})_2]$  with  $\text{NCS}^-$  and Eriochrome Black T ( $\text{EBT}^-$ ) were examined. The protonation reaction results in the transformation of the tetradentate nta to tridentate Hnta. The dissociation of one of the acetic acid moieties is accompanied by the coordination of a third water ligand. A rate constant of  $0.013 \text{ s}^{-1}$  was obtained at  $25^\circ\text{C}$ . The complex ion  $\text{Cr}(\text{nta})(\text{H}_2\text{O})(\text{OH})$  reacts about eight times faster than  $[\text{Cr}(\text{nta})(\text{H}_2\text{O})_2]^-$  with  $\text{NCS}^-$ .  $\text{EBT}^-$  reacts about 16 times faster than  $\text{NCS}^-$ . The stability constants for the products  $\text{Cr}(\text{nta})(\text{H}_2\text{O})(\text{NCS})$  and  $\text{Cr}(\text{nta})(\text{H}_2\text{O})(\text{EBT})$  are 4.60 and 180, respectively [80].

Structural and magnetic studies were performed on the complex  $[\text{Cr}(\text{bispicMe}_2\text{en})(\text{OH})(\text{H}_2\text{O})](\text{ClO}_4)_2$ . A drawing of the tetradentate ligand is shown in (19). The coordination sphere of the Cr(III) centre is octahedral with the pyridine ligands in a *trans* arrangement. The structure exists in dinuclear units in which the hydroxo and aqua ligands are intimately involved in hydrogen bonding interactions with the corresponding ligands of the other complex ion in the asymmetric unit. The average Cr–N(py) distance is 207 pm and the average Cr–N(en) distance is 211 pm. The Cr–O bond lengths are essentially equal and the average is 193 pm. The independent O–Cr–O angles are  $90.2$  and  $89.0^\circ$ . The Cr...Cr separation is 499.9 pm. Magnetic data are consistent with an antiferromagnetic interaction with a singlet ground state. The magnetic moment decreases from  $3.9 \mu_{\text{B}}$  at room temperature to  $0.8 \mu_{\text{B}}$  at 2 K [81].



### 9.4.3.3 Quinquedentate and sexidentate ligands

The complex  $[\text{CrL}(\text{Cl})]\text{ClO}_4 \cdot \text{HClO}_4 \cdot 4\text{H}_2\text{O}$ , where L is (20), has been reported. The structure of  $[\text{CoL}(\text{Cl})]\text{ClO}_4 \cdot 0.75\text{HClO}_4 \cdot 2\text{H}_2\text{O}$  was reported in the same paper. In the Co(III) complex, two (*SS*)-*trans*-cyclohexane-1,2-diamine residues are incorporated into the quinquedentate ligand. The carboxylate group is *trans* to the  $\text{Cl}^-$  ligand. Spectroscopic evidence for the Cr(III) complex suggests that the disposition of the ligands is *cis* [82].



The volume change for the deprotonation of  $[\text{Cr}(\text{edtaH})(\text{H}_2\text{O})]$  was found to be  $2.0 \pm 0.2 \text{ cm}^3 \text{ mol}^{-1}$ . The small value suggests that the formulation of the resultant complex is  $[\text{Cr}(\text{edta})]^-$  rather than  $[\text{Cr}(\text{edta})(\text{H}_2\text{O})]^-$ , i.e., the edta is sexidentate rather than quinquedentate [83].

The reaction between  $[\text{Cr}(\text{en})_3]^{3+}$  and diethylenetriaminepentaacetic acid,  $(\text{AcO})_5\text{dien}$ , has been examined. The en ligands are replaced at a rate that displays an inverse relationship with pH and a direct relationship with  $(\text{AcO})_5\text{dien}$ . A mechanism for the substitution is proposed. The rupture of the three Cr-N chelate rings and the formation of the pentadentate chelate ring is the rate determining step. Activation parameters are reported [84].

A mechanistic study of the periodate oxidation of  $[\text{Cr}(\text{H}_2\text{L})(\text{H}_2\text{O})]^+$ , where  $\text{H}_4\text{L}$  is *N,N,N',N'*-tetraoxalyldiamine, was reported. The rate displays a pH dependence which results from the deprotonation of the ligand and the data suggest that the deprotonated form is the reactive species. The authors suggest that the  $\text{H}_4\text{IO}_6^-$  and  $\text{H}_3\text{IO}_6^{2-}$  anions are the active oxidants and that the process involves an inner-sphere mechanism which proceeds by a one or two electron transfer followed by a fast step to give Cr(VI) [85].

### 9.4.4 Complexes with macrocyclic ligands

Crystal structures and magnetic data have been reported for  $[\text{Cr}(\text{cyclam})(\text{OH})(\text{OH}_2)]\text{ClI}$  and  $[\text{Cr}(\text{cyclam})(\text{OH})(\text{OH}_2)]\text{S}_2\text{O}_6 \cdot 3\text{H}_2\text{O}$ . The structure of  $[\text{Cr}(\text{cyclam})(\text{OH})(\text{OH}_2)]\text{ClI}$  is composed of dinuclear units. The complex cations are related by an inversion centre. The hydroxo and water ligands are *cis* and are involved in a hydrogen bonding network with those on the symmetry related complex cation. The Cr atoms are separated by 492.5 pm. The independent Cr-O bond distances are 197.6 and 193.7 pm. The O-Cr-O angle is  $90.2^\circ$ . Magnetic data suggest that the coupling constant between Cr centers is essentially zero. Solid state EPR data support the magnetic

characterization. Although the cations are disordered in  $[\text{Cr}(\text{cyclam})(\text{OH})(\text{OH}_2)]\text{S}_2\text{O}_6 \cdot 3\text{H}_2\text{O}$ , the structure possesses a similar dimeric structure. The Cr...Cr distance is 503.3 pm [86].

A study of the  $[\text{Cr}(\text{III})(5,5,7,12,12,14\text{-Me}_6\text{cyclam})(\text{OH})(\text{H}_2\text{O})]^{2+}$  catalysed formation of lactic acid was reported. The crystal structure of the product from the reaction with 1,3-dihydroxyacetone,  $[\text{Cr}(\text{Me}_6\text{cyclam})(\text{C}_3\text{H}_4\text{O}_3)]\text{ClO}_4$ , was determined. The macrocycle coordinates in such a way as to leave two *cis* coordination sites open. The compound is a racemic mixture with the (*R*) and (*S*) lactate coordinated to the (*R,R*)- and (*S,S*)- $\text{Me}_6\text{cyclam}$ . A mechanism is proposed for the transformation [87].

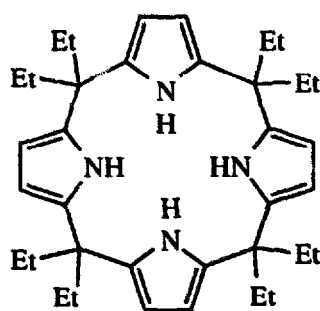
The syntheses and properties of  $\text{Cr}(\text{OH})(\text{py})(\text{Pc})$ , where  $\text{H}_2\text{Pc}$  is phthalocyanine, and  $[\text{Cr}(\text{py})(\text{Pc})]_2\text{O}$  are reported. The room temperature magnetic moments of the monomer and dimer are 3.84 and 1.24  $\mu_B$ , respectively. The UV-VIS spectrum of the dimer displays the characteristic hypsochromic shift with respect to the monomer spectrum. Raman data are reported [88].

The syntheses of a series tetra(*t*-butyl)phthalocyanato,  ${}^t\text{Bu}_4\text{Pc}^{2-}$ , chromium(III) complexes were reported. Evidence is presented that suggests that the complex with the composition  ${}^t\text{Bu}_4\text{PcCrCl}_2\text{H}$  contains the anion  $[{}^t\text{Bu}_4\text{PcCrCl}_2]^-$ , i.e., there is a six-coordinate dichloro complex anion with a  $\text{H}^+$  counterion. The complex is a weak electrolyte in *thf*/MeCN. On reaction with water and hydroxide,  $[\text{Cr}({}^t\text{Bu}_4\text{Pc})]_2\text{O}$  is obtained. On reaction of the salt with pyridine, the complex  $[\text{Cr}(\text{py})_2({}^t\text{Bu}_4\text{Pc})]\text{Cl}$  is obtained [89].

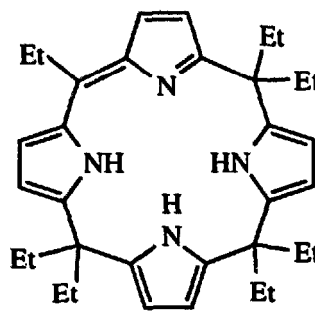
The complexes  $\text{Cr}(\text{TPP})(\text{L})\text{Cl}$  and  $\text{Cr}(\text{TPPOMe})(\text{L})\text{Cl}$ , where *L* = 3- or 4-NOp<sub>y</sub> and  $\text{TPPOMeH}_2$  is tetrakis(4-methoxyphenyl)porphyrin, have been prepared. The Cr(III) centre is involved in an ferromagnetic interaction with the unpaired electron on the 3-NOp<sub>y</sub> ligand, which results in a quintet ground state. However, in the 4-NOp<sub>y</sub> derivatives, an antiferromagnetic interaction is observed with a triplet ground state. The sign of the magnetic interaction is in agreement with that predicted based on the spin polarization mechanism [90, 91].

Pyridine substitution by 1-Melm has been studied for the six-coordinate complex  $\text{Cr}(\text{TPP})(\text{X-py})\text{Cl}$ , where X-py is a substituted pyridine ligand. The rate data are consistent with a mechanism that involves a loss of the py ligand. The five-coordinate complex then reacts with the 1-Melm ligand to give the product. The rate follows a linear free energy relationship with the basicity of the leaving group [92].

The structures of  $\text{Li}_2[\text{Cr}(\text{Et}_8\text{P})(\text{thf})\text{Cl}] \cdot 2\text{thf}$ , where  $\text{H}_4\text{Et}_8\text{P}$  is the porphyrinogen (21), and the two-electron oxidation product  $\text{Cr}(\text{Et}_7\text{P})(\text{thf})_2$ , where  $\text{H}_3\text{Et}_7\text{P}$  is the hemiporphyrin-hemiporphyrinogen (22), were reported. In  $\text{Li}_2[\text{Cr}(\text{Et}_8\text{P})(\text{thf})\text{Cl}] \cdot 2\text{thf}$ , the molecule sits on a *C*<sub>2</sub> axis. The Cl atom is 237 pm from the symmetry related Li atoms and the Cr-Cl bond distance is exceptionally long (243 pm) as a result of the triply bridging bonding mode. The Li atoms are situated above the canted pyrrole rings, which suggests an  $\eta^5$ -pyrrole to Li mode. A final coordination site on the Li is occupied by a *thf* solvate molecule. In  $\text{Cr}(\text{Et}_7\text{P})(\text{thf})_2$ , the macrocycle adopts a flattened saddle shape. The structure is consistent with a delocalized  $\pi$  system in the porphyrin half of the ligand. The average Cr-N(porphyrin) distance, 206 pm, is larger than the average Cr-N(porphyrinogen) distance, 202 pm. The coordination geometry is best described as a distorted octahedron. The Cr-O(*thf*) bond distances are essentially identical at 203.4 and 203.2 pm [93].



$\text{H}_4\text{Et}_8\text{P}$   
(21)



$\text{H}_3\text{Et}_7\text{P}$   
(22)

#### 9.4.5 Dinuclear complexes

*Ab initio* calculations were performed on a linear  $\mu$ -oxo bridged  $\text{CrL}_5$  model system, where the ligands L were model “He-like” atoms with reduced nuclear charge to simulate the coordination of fluoride or ammonia ligands. The coordination geometry about the Cr atoms was octahedral. Comparisons were made with the corresponding Ti(III) and V(III) model compounds. Spin coupling occurs through a superexchange interaction. Paramagnetic (or weak antiferromagnetic) coupling results for the Ti(III) system, but strong ferromagnetic and antiferromagnetic coupling occurs for the V(III) and Cr(III) systems, respectively. These observations agree with experimental findings [94].

Mechanistic investigations of the acid and base hydrolysis reactions on the complexes  $[(\text{tmpa})\text{Cr}(\mu\text{-O})(\mu\text{-RCO}_2)\text{Cr}(\text{tmpa})]^{3+}$ , where tmpa is tris(2-pyridylmethyl)amine, were reported for a wide range of bridging carboxylates. The product of the acid hydrolysis is the bis( $\mu$ -O) complex, but, under conditions of base hydrolysis, the dimer is cleaved to give  $[\text{Cr}(\text{tmpa})(\text{OH})_2]^+$ . The rate of reaction is dependent on the steric demands of the bridging carboxylate and the basicity of the bridge. The rate limiting step for aquation is the breaking of the carboxylate bridge. For the base hydrolysis mechanism, a pre-equilibrium displacement of a tmpa arm by hydroxide is followed by the rate limiting breaking of the carboxylate bridge assisted by a nucleophilic attack of hydroxide [95].

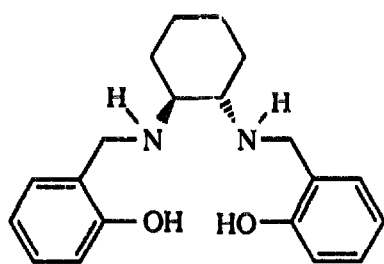
Dinuclear Cr(III)(tacn) complexes, where tacn is 1,4,7-triazacyclononane, with *tris*( $\mu$ -O) or *bis*( $\mu$ -O) and one acetamidato bridges were reported. The salt  $[\text{Cr}(\text{tacn})(\text{H}_2\text{O})_2(\text{OH})][\text{Cr}(\text{tacn})(\text{H}_2\text{O})(\text{OH})_2](\text{TfO})_3 \cdot \text{H}_2\text{O}$  was isolated from a solution of  $[\text{Cr}(\text{tacn})(\text{H}_2\text{O})(\text{OH})_2](\text{TfO})_3$  upon addition of base. The structural assignment of  $[(\text{tacn})\text{Cr}(\text{OH})_3\text{Cr}(\text{tacn})]^{3+}$ , which is formed by the condensation of the complex salt  $[\text{Cr}(\text{tacn})(\text{H}_2\text{O})_2(\text{OH})][\text{Cr}(\text{tacn})(\text{H}_2\text{O})(\text{OH})_2](\text{TfO})_3 \cdot \text{H}_2\text{O}$  in MeCN, is based on spectroscopic evidence (solutions exhibit UV-VIS spectra characteristic of *tris*( $\mu$ -OH) complexes). The crystal structure of  $[(\text{tacn})\text{Cr}(\mu\text{-OH})_2(\mu\text{-MeCONH})\text{Cr}(\text{tacn})]_3 \cdot 3\text{H}_2\text{O}$  was determined. The  $\mu$ -MeCONH causes the  $\text{Cr}_2\text{O}_2$  unit to deviate significantly from planarity. The acetamidato bridge appears to be ordered and displays a similar degree of double-bond character for the C-N and C-O bonds [96].

The heteronuclear complexes  $\text{InCl}_4(\mu\text{-OH})_2\text{Cr(en)}_2$  and  $[\text{TiCl}_4(\mu\text{-OH})_2\text{Cr(en)}_2]\cdot 0.5 \text{H}_2\text{O}$  were studied by X-ray crystallography. In each complex, both of the metals are in octahedral geometries. The In–O–Cr and Ti–O–Cr angles are  $103.7^\circ$  and  $104.5^\circ$ , respectively. The In...Cr and Ti...Cr separations are 323.2 pm and 332.9 pm, respectively [97].

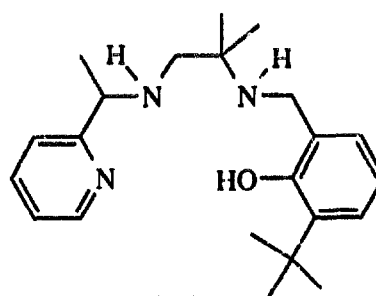
The kinetics of water exchange were reported for  $[(\text{H}_2\text{O})_4\text{Cr}(\mu\text{-OH})_2\text{Cr}(\text{H}_2\text{O})_4]^{4+}$  and  $[(\text{H}_2\text{O})_4\text{Cr}(\mu\text{-OH})_2\text{Cr}(\text{OH})(\text{H}_2\text{O})_3]^{3+}$ . The data suggest that bridging and terminal OH groups have similar effects on the rate of substitution. Also, the aqua groups, both *cis* and *trans*, are labilized upon deprotonation of the dimer [98].

Chromium(III) complexes of saccharides were prepared. The absorption spectra are characteristic of distorted octahedral complexes. The IR spectra suggest that the intermolecular hydrogen-bonding that exists in free solid saccharides is absent in the complexes. EPR spectra are consistent with Cr(III) in an distorted octahedral oxygen field. NMR spectra demonstrate the coordination of simple monosaccharides. The magnetic data are suggestive of a hydroxo bridged dinuclear species ( $J = -9.5 \text{ cm}^{-1}$  for the D-glucose complex). Electrochemical data are also reported [99].

The complexes  $[\text{Cr}([\text{H}_4]\text{salen})\text{Cl}]_2$ ,  $[\text{Cr}(\text{salchd})\text{Cl}]_2$ , and  $\text{Cr}(\text{salpy})\text{Cl}_2$  have been reported.  $[\text{H}_4]\text{salenH}_2$  is tetrahydrosalen. The macrocyclic ligands  $\text{salchdH}_2$  and  $\text{salpyH}$  are represented in (23) and (24). The dinuclear complexes  $[\text{Cr}(\text{salen})\text{Cl}]_2$  and  $[\text{Cr}(\text{salchd})\text{Cl}]_2$  are believed to be structurally related based on the similarity of the magnetic properties. The Cr centers are weakly antiferromagnetically coupled. The structure of the salen complex was determined by X-ray crystallography. The phenolic oxygens bridge the two Cr atoms with a Cr–O–Cr angle of  $79^\circ$ . The Cr–O–Cr angle is  $101^\circ$  and the Cr...Cr distance is 312 pm. The Cr–O distances are 190 and 202 pm and the Cr–N distances are 207 and 206 pm.  $\text{Cr}(\text{salpy})\text{Cl}_2$  displays magnetic properties and an EPR spectrum typical of a mononuclear complex with large zero field splitting [100].

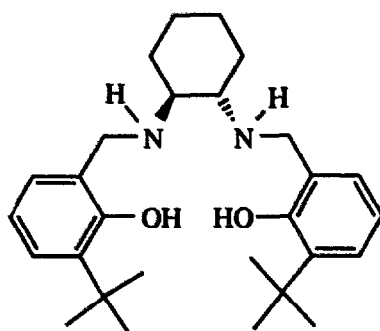


salchdH<sub>2</sub>  
(23)



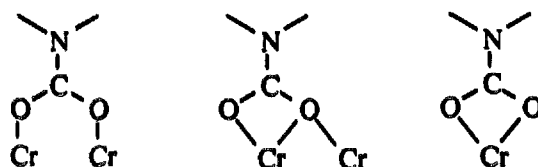
salpyH  
(24)

A fluoro-bridged chromium(III) complex with the macrocyclic ligand shown in (25) has been characterized. The crystal structure of  $\Delta(S,S),\Delta(S,S)-[\{\text{Cr}(\text{salchdbu})\}_2(\mu\text{-fluoro})(\mu\text{-ethoxo})]\cdot \text{H}_2\text{O}$  was reported. The coordination spheres of the two metal centers are distorted octahedra. The Cr–F–Cr and Cr–O–Cr angles are  $103.9^\circ$  and  $101.3^\circ$ , respectively. The Cr–F and Cr–O bond distances are 198 and 201 pm. Magnetic data suggest a weak ferromagnetic coupling between the metal centers [101].



salchdbuH<sub>2</sub>  
(25)

The dinuclear carbamate complex Cr<sub>2</sub>(O<sub>2</sub>CN<sup>i</sup>Pr<sub>2</sub>)<sub>5</sub> has been subjected to a structural analysis using X-ray crystallographic techniques. The carbamate ligands adopt three different bonding modes as shown in (25). Each Cr has a distorted octahedral structure. One of the Cr atoms is bound to six oxygen atoms from the three carbamate ligands. The chloride ligand replaces one of the oxygen atoms for the other Cr. The average Cr–O bond distances for the first and second chromium atoms according to bonding modes shown below are 193.3 and 196.1 pm, 202.1 and 204.2 pm, and 197.9 and 197.5 pm [102].



(26)

The optical charge-transfer (IT) was studied in the ion-paired systems composed of [Fe(CN)<sub>6</sub>]<sup>4–</sup> and [Cr(NH<sub>3</sub>)<sub>6</sub>]<sup>3+</sup> or [Cr(en)<sub>3</sub>]<sup>3+</sup>. The formation of ion pairs was accompanied by the appearance of a band centred at 326 and 339 nm for the hexaammine and tris(en) complexes, respectively. The optical results were compared to [(NH<sub>3</sub>)<sub>5</sub>Cr(μ-NC)Fe(CN)<sub>5</sub>]<sup>–</sup>. In all cases, flash photolysis studies show that MMCT excitation results in a photoredox reaction [103].

The structures of two dinuclear complexes with diphosphinoamido ligands were reported. [Cr<sub>2</sub>Cl<sub>3</sub>{N(CH<sub>2</sub>CH<sub>2</sub>PMe<sub>2</sub>)<sub>2</sub>}{CH<sub>2</sub>P(Me)CH<sub>2</sub>CH<sub>2</sub>NCH<sub>2</sub>CH<sub>2</sub>PMe<sub>2</sub>}]·0.5C<sub>7</sub>H<sub>8</sub> crystallizes with two unique molecules in the asymmetric unit. The two molecules exhibit only minor structural differences. The chromium atoms are each six-coordinate and the Cr···Cr separations are 297 and 299 pm. The octahedra share an edge formed by the two bridging amido nitrogens. One of the methyl groups is deprotonated and involved in a Cr–C σ-interaction. The other coordination sites are occupied by chlorine ligands. The short P–C bond (175 and 177 pm for the two independent distances) indicates some ylide character. The structure of the dinuclear complex [Cr<sub>2</sub>Cl<sub>4</sub>{N(CH<sub>2</sub>CH<sub>2</sub>P<sup>i</sup>Pr<sub>2</sub>)<sub>2</sub>}]<sub>2</sub>·0.5C<sub>7</sub>H<sub>8</sub> was also reported. The two chromium atoms are bridged

by a chlorine atom and two amido nitrogens. The amido ligand adopts a tridentate and a didentate coordination mode in this complex. The Cr...Cr distance is 281 pm and the magnetic data are consistent with two unpaired electrons, suggesting the formation of a Cr-Cr single bond. For the bridging nitrogens, the Cr-N-Cr angles are 85.1 and 84.0°, whereas the Cr-Cl-Cr angle is 71.7° [104].

#### 9.4.6 Polynuclear complexes

The trinuclear,  $\mu^3$ -O complexes  $[\text{Cr}_3\text{O}(\text{O}_2\text{CR})_6\text{L}_3]^+$ , where R is phenyl or tolyl and L is py or  $\text{H}_2\text{O}$ , and  $\text{Cr}_3\text{O}(\text{O}_2\text{CPh})_6(\text{OH})(\text{py})_2$  were reported. One-pot syntheses are reported for each. The crystal structure of  $[\text{Cr}_3\text{O}(\text{O}_2\text{CPh})_6(\text{py})_3]\text{ClO}_4$  was determined. Two crystallographically independent cations are in the asymmetric unit. The cations possess  $C_{3h}$  symmetry and so each set of three Cr atoms is in an equilateral triangle. The coordination geometry of the Cr atoms are distorted octahedra with the py ligands *trans* to the  $\mu^3$ -O, which is situated in the centre of the triangle. The py ligands are perpendicular to the  $\text{Cr}_3\text{O}$  planes. Adjacent Cr atoms are bridged by two benzoate carboxyl groups. The two cations display quite different Cr-O(oxide) and Cr-N bond lengths. In one of the cations, Cr-O(oxide) and Cr-N are 188 and 225 pm, respectively, and in the other cation the corresponding lengths are 190 and 204 pm, respectively. The Cr...Cr distances are 326 and 330 pm. The expected  $^4\text{A}_{2g} \rightarrow ^4\text{T}_{2g}$  and  $^4\text{A}_{2g} \rightarrow ^4\text{T}_{1g}(\text{F})$  bands are observed in the VIS spectra. The IR spectra of the complexes were assigned.  $^1\text{H}$  and  $^2\text{H}$  NMR spectroscopies was used to characterize the complexes. The resonances corresponding to protons in close proximity to the Cr(III) atoms were not observed. Other resonances were paramagnetically shifted. Magnetic susceptibility data are consistent with antiferromagnetically coupled Cr(III) centers resulting in  $S=1/2$  ground states [105].

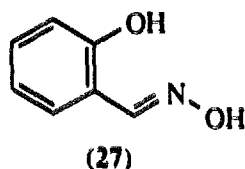
The tetranuclear complex  $[\text{Cr}_4(\mu_3\text{-O})_2(\text{O}_2\text{CMe})_7(\text{phen})_2]\text{Cl} \cdot 1.5\text{CH}_2\text{Cl}_2 \cdot 6\text{H}_2\text{O}$  has been characterized. The cation has  $C_2$  symmetry. The complex possesses a  $\text{Cr}_4\text{O}_2$  core which can be described as a butterfly structure with two edge sharing  $\text{Cr}_3\text{O}$  units. The two Cr atoms on the 'hinge' are bridged by two oxo ligands and have a Cr...Cr separation of 279 pm. They are bridged to the wingtip Cr atom by an oxo ligand. The hinge to wingtip Cr...Cr separations are 330 and 342 pm. Each of the wingtip Cr atoms is coordinated to a phen ligand. The hinge Cr atoms are in a distorted  $\text{O}_6$  octahedral environment, whereas the wingtip Cr atoms are in a distorted  $\text{N}_2\text{O}_4$  octahedral environment. NMR and mass spectral data are reported. Magnetic susceptibility data are consistent with antiferromagnetically coupled Cr atoms in both the solid state and in solution [106].

The complexes  $[\text{Cr}_n\text{Fe}_{n-4}(\mu_3\text{-O})_2(\text{O}_2\text{CMe})_7(\text{bpy})_2]\text{Cl}$  ( $n = 0, 2, 4$ ) have been prepared and characterized. The three complexes are approximately isomorphous. The complex with  $n=2$  has been characterized by X-ray crystallography. The Fe and Cr atoms are disordered. Mössbauer studies support the disorder model with an equal distribution between sites. The data suggest high-spin Fe(III). The  $\text{M}_4\text{O}_2$  core has a butterfly arrangement with the metals in the hinge positions. The third and fourth metal atoms are coordinated to the wingtip oxygen atoms. These metal atoms are coordinated to the bpy ligands. One acetate ligand spans the hinge atoms and the remaining six span

from hinge to peripheral metal. Magnetic data are consistent with antiferromagnetic Fe...Fe and Cr...Fe coupling [107].

The crystal structure of  $\text{Cr}_3(\mu_3\text{-O})(\text{O}_2\text{CNEt}_2)_6\text{Cl}(\text{NH}_2\text{Et})_2$  was reported. The Cr atoms form a trigonal array about the bridging oxo ligand. Adjacent Cr atoms are further bridged by two diethylcarbamato ligands. The octahedral coordination sphere is completed by  $\text{NH}_2\text{Et}$  ligands for two of the Cr atoms and by a chloro ligand for the third. The Cr-O( $\mu_3$ ) distances are 192, 189, and 188 pm. The Cr-O(carbamato) distances range from 196 to 291 pm [108].

The heterometallic complex  $[\text{L}_2\text{Cr}_2(\mu\text{-OMe})_2(\mu_3\text{-O})_2(\text{salox})_2\text{Mn}_2][\text{ClO}_4]_2 \cdot 3\text{H}_2\text{O}$ , where L is (15) and  $\text{H}_2\text{salox}$  is (27), has been characterized. The complex has an  $\text{Mn}_2\text{O}_2$  core which exhibits a butterfly geometry with O wingtips and Mn atoms at the hinge positions and a wing angle of  $135.4^\circ$ . Each oxygen atom is also coordinated to a Cr atom. The cation lies on a two-fold axis which bisects the Mn...Mn vector. The Cr...Cr, Cr...Mn and Mn...Mn distances are 566, 290 and 274 pm, respectively. The Mn-O-Mn and Mn-O-Cr angles are  $94.2^\circ$  and  $98.6^\circ$ , respectively. The two methoxy ligands bridge a Cr and Mn asymmetrically with Cr-O and Mn-O bond distances of 195 and 220 pm, respectively. The bridging, tridentate salox ligands bind to the Mn atoms in didentate fashion employing the phenolic oxygen and the imine nitrogen. The third ligand atom, the deprotonated oxime oxygen, coordinates to the Cr atom. The Mn atoms possess an  $\text{O}_4\text{N}$  coordination sphere. The Mn may be weakly coordinated to a water molecule *trans* to the methoxy ligand (Mn...O = 279 pm). The macrocycle L occupies a face of the distorted octahedral coordination sphere of the Cr atoms. Magnetic measurements reveal a diamagnetic ground state in which antiferromagnetic Mn...Mn and Mn...Cr interactions occur [109].



The results of a spectroscopic investigation of  $[\text{Cr}_3(\mu_3\text{-O})(\text{acr})_6]\text{OH}$  and its polymer, where Hacr is acrylic acid, were reported. The mass spectrum obtained for the monomer is consistent the ascribed formulation. The structure was assigned based on IR spectral data and comparisons with the analogous iron complex. The Cr atoms are believed to form a trigonal array around the bridging oxygen atom. Adjacent Cr atoms are bridged by acrylate ligands. The remaining three acrylate ligands bind in didentate fashion to individual Cr atoms. The polymer is formed by free radical initiation. XPS data for the monomer and polymer were obtained. Evidence is presented that supports a monodentate coordination mode for carboxyl groups in the polymer [110].

The octanuclear mixed-metal clusters  $\text{Na}_2\text{Cr}_2[\text{M}_3\text{O}_4(\text{O}_2\text{CEt})_8]_2$ , where M = Mo or W, was synthesized from  $\text{Na}[\text{M}_3\text{O}_2(\text{O}_2\text{CEt})_9]$  and  $\text{Cr}(\text{CO})_6$  in propionic anhydride. Alternatively, the products were synthesized by reacting  $\text{Na}[\text{M}_3\text{O}_2(\text{O}_2\text{CEt})_9]$ ,  $\text{Mo}(\text{CO})_6$  and  $\text{CrCl}_3 \cdot 6\text{H}_2\text{O}$  or  $\text{Cr}(\text{CO})_6$  and  $\text{Na}_2\text{MO}_4 \cdot 2\text{H}_2\text{O}$ . The crystal structures of the two isostructural compounds were determined. The complexes are composed of two sodium ions and the centrosymmetric dianion  $\text{Cr}_2[\text{M}_3\text{O}_4(\text{O}_2\text{CEt})_8]_2^{2-}$ . The two symmetry related Cr atoms have  $\text{O}_6$  coordination spheres



composed of the oxygens from four bridging propionate ligands and two  $\mu_3$ -oxide ligands, which also bridge two M atoms. The dianion can be considered to be composed of two  $[\text{M}_3\text{O}_4(\text{O}_2\text{CEt})_8]^{4-}$  units bridged by the two Cr ions to form the circular  $\text{Cr}_2[\text{M}_3\text{O}_4(\text{O}_2\text{CEt})_8]^{2-}$  unit. The magnetic properties of these compounds suggest a slight antiferromagnetic coupling of the metal centers. The infrared spectra exhibit three bands in the  $700\text{--}815\text{ cm}^{-1}$  region which are ascribed to the stretching vibrations of the bridging oxygen atoms.  $\text{Na}_2\text{CrFe}[\text{Mo}_3\text{O}_4(\text{O}_2\text{CEt})_8]_2$  was also prepared. Surprisingly, the magnetic data obtained for this compound are suggestive of a ferromagnetic interaction [111].

The syntheses and magnetic susceptibility data were reported for the perchlorate and iodide salts of the cations  $[\text{MO}_4\text{Cr}(\text{cyclam})]_2^{2+}$ , M = Mo and W, and  $[\text{WO}_4\text{Cr}(\text{cyclam})]_4^{4+}$ . The crystal structures of  $[\text{MoO}_4\text{Cr}(\text{cyclam})]_2(\text{ClO}_4)_2$  and  $[\text{WO}_4\text{Cr}(\text{cyclam})]_4(\text{ClO}_4)_4 \cdot 3\text{H}_2\text{O}$  were determined. The structure of the tetrametallic cation is centrosymmetric and contains an essentially planar, eight-membered  $(\text{Mo-O-Cr-O})_2$  ring. The Mo(VI) atoms are tetrahedrally coordinated to the oxide ligands. The two  $\text{MoO}_4$  units bridge the two Cr(cyclam) groups. The symmetry independent Mo-O-Cr angles are  $174^\circ$  and  $148^\circ$ . The Cr(III) ions are in a distorted octahedral  $\text{N}_4\text{O}_2$  environment with an O-Cr-O angle of  $90.3^\circ$ . The  $[\text{WO}_4\text{Cr}(\text{cyclam})]_4^{4+}$  cation has a distorted  $\text{W}_4\text{O}_4$  cube at its centre. Each of the W atoms has a terminal oxide ligand and two oxides which bridge to two different Cr(cyclam) units. The cation has a two-fold axis that passes through two of the Cr atoms. The three symmetry independent O-Cr-O angles range from  $88.1$  to  $89.5^\circ$ . The cyclam ligands adopt a folded configuration in both salts. The magnetic susceptibility of the tetrameric complex varies from  $7.5\text{ }\mu\text{B}$  at room temperature to  $1.6\text{ }\mu\text{B}$  at 4 K. For the dimeric complex, the magnetic susceptibility varies from  $5.4\text{ }\mu\text{B}$  at room temperature to  $4.2$  and  $4.4\text{ }\mu\text{B}$  at 4 K for the iodide and perchlorate salts, respectively. The magnetic data are accounted for using a superexchange model [112].

The crystal structure of the complex  $\text{cis-}[\text{Ru}(\text{bpy})_2(\text{trans-Cr}(\text{cyclam})(\text{CN})_2)_2] \cdot (\text{PF}_6)_3\text{Cl} \cdot 2\text{H}_2\text{O}$  was reported. The bridging CN ligands exhibit Ru-N linkage. The bridging mode was determined from IR spectroscopy. The isomerization of the linkage can be induced thermally, suggesting that the isolated linkage isomer is not the thermodynamically stable one. The Cr-C-N angles are  $170$  and  $172^\circ$  for the bridging CN ligands and  $176$  and  $177^\circ$  for the terminal ligands. The Cr(cyclam) coordination geometry is not remarkable; however, the staggered arrangement of the Cr(cyclam)(CN) groups is unusual [113].

The salts  $[\text{Al}\{(\mu\text{-OH})_2\text{Cr}(\text{en})_2\}_3](\text{S}_2\text{O}_6)_3 \cdot 13\text{H}_2\text{O}$  and  $[\text{In}\{(\mu\text{-OH})_2\text{Cr}(\text{en})_2\}_3](\text{S}_2\text{O}_6)_3 \cdot 6\text{H}_2\text{O}$  were isolated and characterized by X-ray crystallography. The  $[\text{Al}\{(\mu\text{-OH})_2\text{Cr}(\text{en})_2\}_3]^{6+}$  ion has the  $\Delta(\Delta\Delta\Delta)$  configuration. The Al-O bond distances range from  $188$  to  $191\text{ pm}$ . The average Cr-O and Cr-N bond lengths are  $193$  and  $206\text{ pm}$ , respectively. The Al-O-Cr angles range from  $100.5$  to  $101.7^\circ$ . The O-Al-O and O-Cr-O angles range from  $79.4$  to  $79.8^\circ$  and  $77.6$  to  $77.9^\circ$ , respectively. The  $[\text{In}\{(\mu\text{-OH})_2\text{Cr}(\text{en})_2\}_3]^{6+}$  ion has the  $\Delta(\Delta\Delta\Delta)$  configuration. The In-O distances range from  $213$  to  $219\text{ pm}$ . The average Cr-O and Cr-N bond lengths are  $195$  and  $208\text{ pm}$ . The In-O-Cr angles range from  $101.2$  to  $103.7^\circ$ . The O-In-O and O-Cr-O angles range from  $71.5$  to  $72.4^\circ$  and  $79.6$  to  $81.5^\circ$ , respectively [114].

The syntheses of salts with pairs of  $\mu$ -oxo or  $\mu$ -hydroxo bridged Cr(tpma) units, where tpma is *tris*(2-pyridylmethyl)amine, which are in turn bridged by succinate or malonate ligands were reported. Upon diprotonation, the cation of the salt  $[(\mu\text{-O}_2\text{C}(\text{CH}_2)_n\text{CO}_2)\{(\text{tpma})\text{Cr}(\mu\text{-O})\text{Cr}(\text{tpma})\}_2](\text{ClO}_4)_6 \cdot 4\text{H}_2\text{O}$  ( $n = 1$  or  $2$ ) yields  $[(\mu\text{-O}_2\text{C}(\text{CH}_2)_n\text{CO}_2)\{(\text{tpma})\text{Cr}(\mu\text{-OH})\text{Cr}(\text{tpma})\}_2]^{8+}$ . The salts  $[(\text{tpma})\text{Cr}(\mu\text{-O})(\mu\text{-O}_2\text{C}(\text{CH}_2)_2\text{CO}_2)\text{Cr}(\text{tpma})](\text{ClO}_4)_2 \cdot 6\text{H}_2\text{O}$  and  $[(\text{tpma})\text{Cr}(\mu\text{-OH})(\mu\text{-O}_2\text{C}(\text{CH}_2)_2\text{CO}_2\text{H})\text{Cr}(\text{tpma})](\text{ClO}_4)_4 \cdot 5\text{H}_2\text{O}$ , in which the succinate bridges through a single carboxylate group, were also prepared [115].

The complexes  $[\text{Cr}(\text{[H}_4\text{]salen})\text{F}]_4$  and  $[\text{Cr}(\text{salchd})\text{F}]_4 \cdot 2\text{H}_2\text{O}$ , where  $[\text{H}_4]\text{salenH}_2$  is tetrahydrosalen and  $\text{salchdH}_2$  is shown in (23), were synthesized from the free-base ligands and *trans*- $[\text{Cr}(\text{py})_4\text{F}_2]\text{ClO}_4$ . The crystal structure of  $[\text{Cr}(\text{[H}_4\text{]salen})\text{F}]_4$  reveals discrete tetranuclear units with F bridges. The Cr atoms are in an octahedral environment with the  $\text{O}_2\text{N}_2$   $[\text{H}_4]\text{salen}^{2-}$  occupying four sites and the  $\text{F}^-$  ligands *cis*. This results in an eight-membered ring with alternating Cr and F atoms. A two-fold axis passes through the centre of the ring. The arrangement of the tetradentate ligands around the Cr centers is  $\Delta\Delta\Delta\Delta$ . The closest Cr...Cr distance is 373 pm. The mean Cr-F-Cr and F-Cr-F angles are 149.2 and 89.7°, respectively. The Cr-F bond distances range from 192.5 to 194.5 pm. The ranges for the Cr-N and Cr-O distances are 201 to 207 pm and 189 to 193 pm, respectively. The two complexes display essentially identical magnetic character. The Cr atoms are antiferromagnetically coupled, albeit weakly. Based on mass spectral, EPR spectroscopic, and magnetic data,  $[\text{Cr}(\text{salchd})\text{F}]_4 \cdot 2\text{H}_2\text{O}$  has fluoride bridges and has a structure similar to  $[\text{Cr}(\text{[H}_4\text{]salen})\text{F}]_4$  [116].

The complex  $[\text{Mo}_3\text{CrS}_4(\text{H}_2\text{O})_{12}]^{4+}$  has been prepared and shown to possess a heterometallic cuboidal structure. The presence of the sulfur labilizes the Cr(III). The 4+ charge was confirmed by the stoichiometry of the oxidation of the cluster with  $\text{Fe}^{3+}$  and  $[\text{Co}(\text{dipic})_2]^-$ . With each, a three-equivalent conversion of  $[\text{Mo}_3\text{CrS}_4(\text{H}_2\text{O})_{12}]^{4+}$  to  $[\text{Mo}_3\text{S}_4(\text{H}_2\text{O})_9]^{4+}$  and  $\text{Cr}(\text{H}_2\text{O})_6^{3+}$  occurs. The mechanism appears to be outer-sphere. The substitution of water coordinated to Cr with  $\text{NCS}^-$  was studied by stopped-flow techniques. The substitution is 1:1 water: $\text{NCS}^-$ . The observed dependence on pH is consistent with the conjugate-base mechanism [117].

The complexes  $[\text{Cr}_{3-x}\text{Fe}_x\text{O}(\text{O}_2\text{CR})_6(\text{H}_2\text{O})_3]\text{NO}_3$  ( $x = 1, 2$ ;  $\text{R} = \text{Me, Et, Ph}$ ) have been reexamined. Findings from  $^1\text{H}$ -NMR and mass spectroscopic studies show that the complexes previously formulated as heterotrimeric carboxylates of Cr(III) and Fe(III) are actually mixtures of the heteronuclear species and homonuclear species. The authors demonstrated that the distribution of products is not purely statistical, but rather reflects the relative reactivity of Cr(III) and Fe(III) [118].

The compounds with the formulas  $(\text{NH}_4)_2[\text{Cr}_2\text{M}(\text{tart})_4] \cdot 4\text{H}_2\text{O}$ ,  $\text{M} = \text{Cu(II)}$  or  $\text{Co(II)}$ , were prepared. The complexes were characterized by IR and UV-VIS spectroscopies and elemental, magnetic and thermogravimetric analyses. IR spectral data suggest coordination of the hydroxy groups. The Co(II) compound exhibits a UV-VIS spectrum with three bands, two attributed to the Cr(III) and one to the Co(II), suggesting octahedral coordination for both Cr(III) and Co(II). The magnetic data is suggestive of a weak antiferromagnetic interaction between metal centers. The products obtained after thermal decomposition at 660° give X-ray spectra indicative of the

formation of copper chromite with an inverse spinellic structure and cobalt chromites with a normal spinellic structure [119].

Simplified procedures for the synthesis of salts of the Cr(III) heteropolymetallates  $\alpha$ -[PW<sub>11</sub>O<sub>39</sub>Cr(OH<sub>2</sub>)]<sup>4-</sup> and  $\alpha_2$ -[P<sub>2</sub>W<sub>17</sub>O<sub>61</sub>Cr(OH<sub>2</sub>)]<sup>7-</sup> and their oxidation to the Cr(V) heteropolymetallates  $\alpha$ -[PW<sub>11</sub>O<sub>39</sub>CrO]<sup>4-</sup> and  $\alpha_2$ -[P<sub>2</sub>W<sub>17</sub>O<sub>61</sub>CrO]<sup>7-</sup> were reported. The Cr(V) anions can be prepared by electrochemical or chemical oxidation. Cyclic voltammetric and controlled-potential electrolysis measurements were performed. The results are consistent with oxidation occurring in a two-electron step. EPR spectra of the Cr(V) salts show a strong signal with an isotropic *g* value of 1.956. Attempts to oxidize the Cr(V) to Cr(VI) were unsuccessful. Attempts to reduce the Cr(III) to Cr(II) resulted in the reduction of the tungsten-oxo cage. The diffusion coefficients for the chromium substituted anions were determined by rotating disk voltammetry. The hydrodynamic radii determined from the average diffusion coefficients are 540 and 890 pm for  $\alpha$ -[PW<sub>11</sub>O<sub>39</sub>Cr(OH<sub>2</sub>)]<sup>4-</sup> and  $\alpha_2$ -[P<sub>2</sub>W<sub>17</sub>O<sub>61</sub>Cr(OH<sub>2</sub>)]<sup>7-</sup>, respectively, which, when compared to the crystallographic radii, suggest that the anions are not strongly hydrated [120].

The first example of a triply substituted Keggin anion containing low-valent heteroatoms was reported. The structure of K<sub>3</sub>H<sub>4</sub>[A- $\alpha$ -SiO<sub>4</sub>W<sub>9</sub>Cr<sub>3</sub>(OH<sub>2</sub>)<sub>3</sub>O<sub>33</sub>] was determined by X-ray crystallography. One of the Cr atoms is on a mirror plane and the other two are in general positions. The Cr atoms are in an almost ideal O<sub>6</sub> octahedral environment. Each Cr atom is coordinated to a terminal water ligand and to five bridging oxides. Some of the more interesting structural features include short Cr...W distances, an inter anionic Cr...Cr distance of 528 pm, and an intra anionic Cr...Cr distance of 578 pm [121].

Reaction of SCl<sub>2</sub> or S<sub>2</sub>Cl<sub>2</sub> with [Cr(acac)<sub>2</sub>(tfac)] or [Cr(acac)<sub>2</sub>(acac-CHO)], where tfac is 1,1,1-trifluoroacetylacetonate and acac-CHO is 3-formylacetylacetonate, results in the formation of polymers with Cr(III) incorporated in the backbone. The products were characterized by their viscosities, FTIR spectra and gel permeation chromatography. The molecular weights were estimated [122].

## 9.5 CHROMIUM(II)

### 9.5.1 Mononuclear complexes

The tetra-*n*-butylammonium salt of tetrakisothiocyanatochromate(II) crystallizes in two forms. One form is composed of discrete square-planar [Cr(NCS)<sub>4</sub>]<sup>2-</sup> anions with a crystallographically imposed centre of symmetry. The mean Cr-N bond distances are 201.2 and 201.0 pm and the Cr-N-C bond angles are 173.5 and 175.4°. The effective magnetic moment is 4.76  $\mu_B$  and is temperature independent to 177 K. The second form exhibits a temperature dependent magnetic moment which decreases from 4.30  $\mu_B$  at room temperature to 3.36  $\mu_B$  at 90 K. The complex anion exists in the form of loose dimers with two NCS<sup>-</sup> bridges. The resulting coordination geometry can be described as a square-pyramid with trigonal-bipyramidal distortion. The coordination sphere is composed of isothiocyanato ligands in the basal plane and a weak interaction with the sulfur end of an NCS<sup>-</sup> from an adjacent anion. The Cr-N bond distances range from 200.9 to 201.6 pm. The Cr-S distance is 272 pm. The N-Cr-S and N-Cr-N angles range from

84.2 to 107.7° and 90.6 to 91.4°. The Cr–N–C angles are in the range 164 to 178°. The Cr...Cr distance is 583.7 pm and the magnetic data is fit well with a model in which magnetic interactions are only considered between Cr atoms in a given dimeric pair [123].

The structures of solid solutions  $(\text{NH}_4)_2[\text{Cr}_{0.10}\text{Zn}_{0.90}(\text{H}_2\text{O})_6](\text{SO}_4)_2$  and  $(\text{NH}_4)_2[\text{Cr}_{0.22}\text{Zn}_{0.78}(\text{H}_2\text{O})_6](\text{SO}_4)_2$  were determined using single-crystal neutron and X-ray diffraction analysis. The asymmetric unit of the isomorphous structures contains one ammonium ion, one sulfate ion, and one-half  $[\text{Cr}/\text{Zn}(\text{H}_2\text{O})_6]^{2+}$  ion. An extensive hydrogen-bonding network constrains the environment of the complex ion. The results demonstrate disorder in the Jahn-Teller induced distorted aqua ligand. Whether the disorder is static, dynamic, or both could not be discerned from the data. The disorder was apparent in the room temperature X-ray results, but was more apparent in the low-temperature neutron data [124].

In the reduction of chromate with DL-penicillamine, L-cysteine, and glutathione,  $\text{Cr}^{2+}$  was detected as an intermediate. The intermediacy of  $\text{Cr}^{2+}$  was demonstrated by monitoring the formation of superoxochromium(III) via the reaction of the  $\text{Cr}^{2+}$  with dioxygen [125].

The effect of oxyanion concentration, temperature and pressure on the hydrogen peroxide oxidation of Cr(II) was examined. The results suggest that  $\text{Cr}(\text{H}_2\text{O})_6^{2+}$  and  $\text{Cr}(\text{An})(\text{H}_2\text{O})_5^+$ , where An is a coordinated oxyanion, rapidly coordinate  $\text{H}_2\text{O}_2$  followed by a rapid inner-sphere, rate-determining electron-transfer reaction. The presence of the anion in the coordination sphere promotes either the formation of the inner-sphere complex, the electron-transfer process, or both. An examination of activation volumes suggests that the anion-induced electron-transfer involves a lengthening of the O–O bond, which promotes bond cleavage, as a result of the increase in electron density at the metal centre [126].

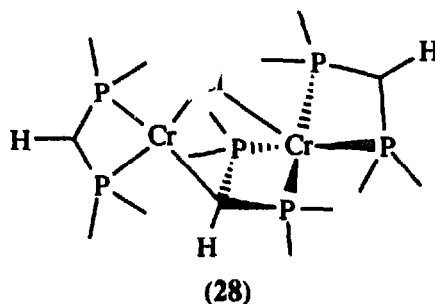
The chain decomposition reaction of  $[\text{Ti}(\text{O}_2)(\text{ox})_2]^{2-}$  and Ti(III) initiated by Cr(II) was studied. Reaction (vi) was monitored and the reaction rate constant was found to be  $2.5 \times 10^4 \text{ mol}^{-1} \text{ dm}^3 \text{ s}^{-1}$ . The result for Ti(III) was similar. The chain length increased with an increase in the amount of added oxylate ion. Oxygen is an inhibitor of the chain reaction. EPR spectroscopy was used to study the formation  $\cdot\text{OH}$  using the spin-trapping technique. The maximum value of the chain length was found to be 490 units under the experimental conditions used [127].



### 9.5.2 Dinuclear complexes

A dinuclear complex with a bridging chloride and bridging didentate bis(diphenylphosphino)methanide ligand has been isolated.  $[\text{Cr}(\text{Ph}_2\text{PC}(\text{H})\text{PPh}_2)(\mu\text{-Cl})[\mu\text{-C}(\text{H})(\text{PPh}_2)_2][\text{Cr}(\text{Ph}_2\text{PC}(\text{H})\text{PPh}_2)]$  was prepared from  $\text{CrCl}_2(\text{thf})_2$  and  $[\text{Ph}_2\text{PC}(\text{H})\text{PPh}_2]\text{Li}$ . The compound crystallizes with one and one-half molecules of toluene and one-half molecule of thf. The crystal structure of the compound reveals one tetra-coordinated and one penta-coordinated Cr(II) atom. The square-planar Cr is coordinated to a didentate ligand, the bridging chloride, and the methanide carbon of the diphosphine (Cr–C = 220 pm) which is in turn coordinated to the square-pyramidal Cr in a didentate fashion, as seen in (28). The square-pyramidal coordination sphere of

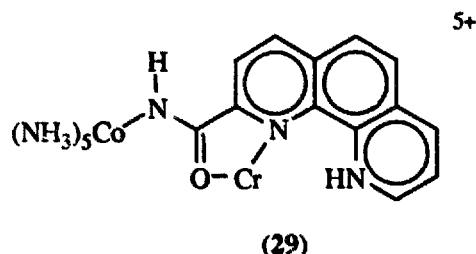
the Cr atom is completed with a non-bridging diphosphine ligand and the bridging Cl in the apical position. The Cr...Cr distance is 371 pm. The magnetic moment is  $6.07\mu_B$  per dinuclear unit and, surprisingly, the complex is EPR silent [128].



Structural and magnetic data were reported for the complexes  $\{[(\text{Ph}_2\text{PCH}_2\text{SiMe}_2)_2\text{N}]\text{Cr}\}_2(\mu\text{-Cl})_2$  and  $\{[(\text{Ph}_2\text{PCH}_2\text{SiMe}_2)_2\text{N}]\text{Cr}\}_2(\mu\text{-H})_2$ . Although the chromium centers are antiferromagnetically coupled in both complexes, the degree of interaction is much stronger when the bridging units are hydrides rather than chlorides ( $J = -12.4$  and  $-139\text{ cm}^{-1}$ , respectively). The structures of each were reported. The Cr atoms and the Cl atoms in  $\{[(\text{Ph}_2\text{PCH}_2\text{SiMe}_2)_2\text{N}]\text{Cr}\}_2(\mu\text{-Cl})_2$  are related by a centre of symmetry and have a slightly distorted trigonal-bipyramidal geometry with the amido nitrogen in an axial site and the two phosphines in equatorial sites. The coordination geometry is completed with bridging chlorides in the remaining axial and equatorial site. The Cr...Cr separation is 364 pm and the Cr-Cl bond distances are 239.7 and 254.6 pm for the axial and equatorial chlorides, respectively. The N-Cr-Cl(ax) and N-Cr-Cl(eq) angles are  $179.2^\circ$  and  $94.8^\circ$ . The Cr-Cl-Cr angle is  $94.6^\circ$ . The structure of  $\{[(\text{Ph}_2\text{PCH}_2\text{SiMe}_2)_2\text{N}]\text{Cr}\}_2(\mu\text{-H})_2$  is quite similar but the smaller bridging hydrides result in greater distortions from trigonal-bipyramidal geometry. The Cr...Cr separation is 264 pm, considerably shorter than in the corresponding chloride complex and within bonding distance. The Cr-H bond distances are 178 and 176 pm for the axial and equatorial hydrides, respectively. The Cr-H-Cr angle is  $83^\circ$  [129].

The preparation of  $[\text{Cr}(\text{NH}_3)_5(\text{NHCO-phen})]^{3+}$ , (NH<sub>2</sub>CO-phen is 1,10-phenanthroline-2-carboxamide) and its reduction by Cr(II) were reported. The reduction proceeds via the formation of the intermediate shown below, (29). The reaction follows the rate law shown in equation (vii) where  $K_p$  is the formation constant of the dinuclear species and  $k_{et}$  is the intramolecular electron-transfer rate constant.  $K_p = 28\text{ M}^{-1}$  and  $k_e = 140\text{ s}^{-1}$  at  $25^\circ\text{C}$ . Complete transfer of the bridging ligand was observed [130].

$$k_{obs} = K_p k_{et} [\text{Cr}^{2+}] / (1 + K_p [\text{Cr}^{2+}]) \quad (\text{vii})$$



### 9.5.3 Polynuclear complexes

The polymeric compound  $[\text{Cr}(\text{N}_2\text{H}_2\text{Ph}_2)_2\text{Cl}_2]_n$  was synthesized from diphenylhydrazine and anhydrous  $\text{CrCl}_2$ . The complex is insoluble in polar and nonpolar substances. The elemental analysis for this compound was marginal. The IR spectrum is suggestive of a bridging didentate linkage and the reflectance spectrum is consistent with an octahedral environment. The magnetic moment at room temperature is  $4.82 \mu_B$  [131].

The crystallization from a reaction medium of aqueous  $\text{CrSO}_4$  and pyridine gave the chain type compound  $[(\text{H}_2\text{O})_2(\text{py})_2\text{CrSO}_4\text{Cr}(\text{py})_4\text{SO}_4]_{\infty} \cdot 4_{\infty}\text{H}_2\text{O}$  at low temperature and the tetranuclear compound  $[\text{Cr}(\text{SO}_4)(\text{OH})(\text{py})_2]_4 \cdot 2\text{H}_2\text{O}$  at room temperature. In the chain type compound, the two chromium atoms have different coordination spheres. Each resides on an inversion centre and the chromium atoms are bridged by O-S-O linkages from sulfate ligands. One of the chromium atoms completes its coordination sphere with four pyridine ligands and the other chromium atom has two water ligands and two pyridine ligands. Jahn-Teller distorted Cr-O(water) and Cr-O(sulfato) bond lengths (227 and 246 pm, respectively) are significantly longer than the Cr-N bond distances (214 pm for the Cr with two pyridine ligands and 214 and 222 for the Cr with four pyridine ligands). Due to the presence of a four-fold axis, the four Cr atoms are equivalent in the tetranuclear complex. Each is coordinated in an octahedral fashion by two pyridine ligands, two bridging hydroxo ligands, and two oxygen atoms from bridging sulfato ligands. Water molecules form hydrogen bonds to oxygen atoms of alternate sulfato groups. This is the first reported incidence of this structural type. The average Cr-O(hydroxo), Cr-O(sulfato), and Cr-N bond distances are 196, 195, and 211 pm, respectively [132].

### REFERENCES

1. E.S. Gould, *Coord. Chem. Rev.*, 135/136 (1994) 651.
2. E. Zinato, *Coord. Chem. Rev.*, 129 (1994) 195.
3. D.A. House, *Mech. Inorg. Organomet. React.*, 8 (1994) 97.
4. J.F. Perez-Benito, D. Lamrhari and C. Arias, *J. Phys. Chem.*, 98 (1994) 12621.
5. J.F. Perez-Benito, C. Arias, D. Lamrhari and A. Anhari, *Int. J. Chem. Kin.*, 26 (1994) 587.
6. S.R. Signorella, M.I. Santoro, M. Mulero and L.F. Sala, *Can. J. Chem.*, 398 (1994) 398.
7. J.F. Perez-Benito, D. Lamrhari and C. Arias, *Can. J. Chem.*, 72 (1994) 1637.
8. M. Mousavi, H. Firouzabadi and M. Shamsipur, *Int. J. Chem. Kinetics*, 26 (1994) 497.
9. R. Castano, M.A. Olazabal, G. Borge and J.M. Madariaga, *J. Chem. Soc., Faraday Trans.*, 90 (1994) 1227.

10. J. Sundermeyer, J. Putterlik, M. Foth, J.S. Field and N. Ramesar, *Chem. Ber.*, 127 (1994) 1201.
11. G.M. Larin, G.A. Zvereva and V.V. Minin, *Koord. Khim.*, 20 (1994) 827.
12. B. Nair, M. Kanthimathi, K. Raj and T. Ranasami, *Proc. Indian Acad. Sci., Chem. Sci.*, 106 (1994) 681.
13. N. Azuma, T. Ozawa and S. Tsuboyama, *J. Chem. Soc., Dalton Trans.*, (1994) 2609.
14. A. Al-Ajouni, A. Bakac and J.H. Espenson, *Inorg. Chem.*, 33 (1994) 1011.
15. S. Milicev, K. Lutar, B. Zemva and T. Ogrin, *J. Mol. Struct.*, 323 (1994), 1.
16. B. Nair, M. Kanthimathi, K. Raj and T. Ranasami, *Proc. Indian Acad. Sci., Chem. Sci.*, 106 (1994) 681.
17. A. Døssing, *Acta Chem. Scand.*, 48 (1994) 269.
18. S. Kaizakis and J.I. Legg, *Inorg. Chim. Acta*, 218 (1994) 179.
19. T. Schönherr, R. Wiskemann and D. Mootz, *Inorg. Chim. Acta*, 221 (1994) 93.
20. S. Suma, M.R. Sudarsanakumar, C.G.R. Nair and C.P. Prabhakaran, *Indian J. Chem.*, 33A (1994) 775.
21. S. Suma, M.R. Sudarsanakumar, C.G.R. Nair and C.P. Prabhakaran, *Indian J. Chem.*, 33A (1994) 1107.
22. C. Guran, I. Jitaru and I. Ciocoiu, *Rev. Roum. Chim.*, 39 (1994) 291.
23. M. Prien, G. Koske and H.J. Seifert, *Z. Anorg. Allg. Chem.*, 620 (1994) 1943.
24. G. González, B. Moullet, M. Martinez and A.E. Merbach, *Inorg. Chem.*, 33 (1994) 2330.
25. M. Rievag, D. Bustin, J. Mocák, R. Riccieri and E. Zinato, *Inorg. Chim. Acta*, 216 (1994) 113.
26. Y. Chen, D.H. Christensen, G.O. Sørensen, O.F. Nielsen, C.H.H. Jacobsen and J. Hyldtoft, *J. Mol. Struct.*, 319 (1994) 138.
27. A. Bakac, J.H. Espenson and J.A. Janni, *J. Chem. Soc., Chem. Commun.*, (1994) 315.
28. C. Kang and F.C. Anson, *Inorg. Chem.*, 33 (1994) 2624.
29. J. H. Espenson, A. Bakac and J. Janni, *J. Am. Chem. Soc.*, 116 (1994) 3436.
30. I. Pollini, *Phys. Rev. B: Condens. Matter*, 50 (1994) 2095.
31. J. Suh, H. Shin, C. Yoon, K. Lee, I. Suh, J. Lee, B. Ryu and S. Li, *Bull. Korean Chem. Soc.*, 15 (1994) 245.
32. A. Sekine, T. Otsuka, Y. Ohashi and Y. Kaizu, *Acta Crystallogr., Sect. C*, 50 (1994) 1399.
33. H. Sakane, I. Watanabe, Y. Yokoyama, S. Ikeda and T. Taura, *Polyhedron*, 13 (1994) 1625.
34. U. Bossek, G. Haselhorst, S. Ross, K. Wiegardt and B. Nuber, *J. Chem. Soc., Dalton Trans.*, (1994), 2041.
35. V.A. Reutov and E.V. Gukhman, *Zh. Obshch. Khim.*, 64 (1994) 889.
36. H. Zheng and T.M. Swager, *J. Amer. Chem. Soc.*, 116 (1994) 761.
37. C.A. Blanco and J. Sumillera, *New J. Chem.*, 18 (1994) 223.
38. H. Oki, Y. Kitagawa and R. Nakata, *Bull. Chem. Soc. Jpn.*, 67 (1994) 1825.
39. B.M.A. El-Khair, S.M. Mokhtar, A.Z. Dakroury and M.B.S. Osman, *J. Macromol. Sci., Phys.*, B33 (1994) 387.
40. A.K.A. El-Hadi, S.A. Helmy and M.A. Abou-State, *Transition Metal Chem.*, 19 (1994) 340.
41. H. El-Saied, A.H. Basta, A.K. Abdel-Hadi and W.M. Hosny, *Polym. Int.*, 35 (1994) 27.
42. J. Petrova, Z. Zdravkova, O. Angelova, and J. Macicek, *J. Coord. Chem.*, 33 (1994) 161.
43. C.R.A. Rajendram and P.E. Hoggard, *J. Coord. Chem.*, 33 (1994) 15.
44. M.C. Morón, F. Palacio, J. Pons, J. Casabó, X. Solans, K.E. Merabet, D. Huang, X. Shi, B.K. Teo and R.L. Carlin, *Inorg. Chem.*, 33 (1994) 746.
45. O. Grancicová and M. Lezovic, *Transition Metal Chem.*, 19 (1994) 465.
46. K. Kurzak and A. Kolkowicz, *Pol. J. Chem.*, 68 (1994) 1501.
47. J. Choi, *Bull. Korean Chem. Soc.*, 15 (1994) 145.
48. A.D. Kirk and S.R.L. Fernando, *Inorg. Chem.*, 33 (1994) 4435.
49. A. D. Kirk and A. M. Ibrahim, *Inorg. Chem.*, 29 (1990) 4848.

50. C.C. Mukhopadhyay and G.S. De, *Transition Metal Chem.*, **19** (1994) 49.
51. A.K.A. Hadi, *Indian J. Chem., Sec. A.*, **33A** (1994) 879.
52. G.A. Gnanaraj, S. Rajagopal and C. Srinivasan, *Tetrahedron*, **50** (1994) 9447.
53. H. Riesen, E. Krausz and L. Dubicki, *Chem. Phys. Lett.*, **218** (1994) 579.
54. M.A. Watzky, X. Song, J.F. Endicott, *Inorg. Chim. Acta*, **226** (1994) 109.
55. C. Pizzocaro, M. Bolte, H. Sun and M.Z. Hoffman, *New J. Chem.*, **18** (1994) 737.
56. H. Okawa, M. Mitsumi, M. Ohba, M. Kodera and N. Matsumoto, *Bull. Chem. Soc. Jpn.*, **67** (1994) 2139.
57. B.S. Garg, R.K. Garg and M.J. Reddy, *J. Coord. Chem.*, **33** (1994) 109.
58. H. Oki, K. Katou, S. Shinbashi, H. Kawamura and R. Nakata, *Synth. React. Inorg. Met.-Org. Chem.*, **24** (1994) 9.
59. G.M.A. El-Reash, I.M.M. Kenawy, U. El-Ayaan and M.A. Khattab, *Indian J. Chem., Sect. A*, **33A** (1994) 914.
60. A.A. Razik and A.K.A. Hadi, *Transition Metal Chem.*, **19** (1994) 84.
61. C.C. Mukhopadhyay and G.S. De, *Indian J. Chem., Sect. A*, **33A** (1994) 664.
62. Mazhar-ul-Haque and M.S. Hussain, *Transition Metal Chem.*, **19** (1994) 95.
63. S.D. Dhumwad, K.G. Gudasi and T.R. Goudar, *Indian J. Chem., Sect. A*, **33A** (1994) 320.
64. L. Armiho and V. Arancibia, *Anal. Chim. Acta*, **298** (1994) 91.
65. P.D. Sawalakhe, M.L. Narwade and K.N. Wadodkar, *J. Indian Chem. Soc.*, **71** (1994) 49.
66. B. Gulanowski, M. Cieslak-Golanka, K. Szyba and J. Urban, *Biometals*, **7** (1994) 177.
67. V. Subramaniam and P.E. Hoggard, *J. Coord. Chem.*, **31** (1994) 157.
68. D. House, S. Schaffner, R. van Eldik, A. McAuley and M. Zhender, *Inorg. Chim. Acta*, **277** (1994) 11.
69. V. Subramaniam, K. Lee and P.E. Hoggard, *Inorg. Chim. Acta*, **216** (1994) 155.
70. V. Subramaniam and P.E. Hoggard, *J. Inorg. Biochem.*, **54** (1994) 49.
71. C.R.A. Ragendram and P.E. Hoggard, *J. Coord. Chem.*, **33** (1994) 15.
72. M.Z. A. Rafiquee, Z.K. Khan and A.A. Khan, *Transition Metal Chem.*, **19** (1994) 477.
73. P. Sonawane, R. Chikate, A. Kumbhar and S. Padhye, *Polyhedron*, **13** (1994) 395.
74. H. Heaster and P.E. Hoggard, *Polyhedron*, **13** (1994) 333.
75. A.R.H. Al-Soudani, A.S. Batsanov, P.G. Edwards and J.A.K. Howard, *J. Chem. Soc., Dalton Trans.*, (1994) 987.
76. A.D. Kirk and S.R.L. Fernando, *Coord. Chem. Rev.*, **132** (1994) 121.
77. A.D. Kirk and S.R.L. Fernando, *Inorg. Chem.*, **33** (1994) 4041.
78. P.J. Toscano, T.T. DiMauro, S. Geremia, L. Randaccio and E. Zangrundo, *Inorg. Chim. Acta*, **217** (1994) 195.
79. K. Dey and K. Chakraborty, *Indian J. Chem., Sec. A*, **33A** (1994) 679.
80. H.G. Visser, J.G. Leipoldt, W. Purcell and D. Mostert, *Polyhedron*, **13** (1994) 1051.
81. P.A. Goodson, J. Glerup, D.J. Hodgson, K. Michelsen and U. Rychlewska, *Inorg. Chem.*, **33** (1994) 359.
82. T.W. Hambley, G.A. Lawrance, M. Maeder and G. Wei, *J. Chem. Soc., Dalton Trans.*, (1994) 355.
83. K. Yoshitani, *Bull. Chem. Soc. Jpn.*, **67** (1994) 2115.
84. V. Garg, S. Kumar and P.S. Relan, *Orient. J. Chem.*, **10** (1994) 35.
85. A.A. Abdel-Khalek, S.M. Sayyah and F.F. Abdel-Hameed, *Transition Metal Chem.*, **19** (1994) 108.
86. P.A. Goodson, J. Glerup, D.J. Hodgson, K. Michelsen and U. Rychlewska, *Inorg. Chem.*, **33** (1994) 359.
87. E. Band, J. Eriksen and L. Mønsted, *Acta Chem. Scand.*, **48** (1994) 12.
88. S. Sievertsen and H. Homborg, *Z. Anorg. Allg. Chem.*, **620** (1994) 1601.
89. M. Bode and F. Wasgestian, *Inorg. Chim. Acta*, **224** (1994) 185.
90. M. Kitano, N. Koga and H. Iwamura, *J. Chem. Soc., Chem. Commun.*, (1994) 447.
91. M. Kitano, Y. Ishimaru, K. Inoue, N. Koga and H. Iwamura, *Inorg. Chem.*, **33** (1994) 6012.



92. M. Inamo, S. Sugiura, H. Fukuyama and S. Funahashi, *Bull. Chem. Soc. Jpn.*, 67 (1994) 1848.
93. E. Solari, F. Muso, C. Floriani, A. Chiesi-Villa and C. Rizzoli, *J. Chem. Soc., Dalton Trans.*, (1994) 2015.
94. K. Fink, R. Fink and V. Staemmler, *Inorg. Chem.*, 33 (1994) 6219.
95. T.F. Tekut and R.A. Holwerda, *Inorg. Chem.*, 33 (1994) 5254.
96. P. Andersen, H. Matsui, K.M. Nielsen and A.S. Nygaard, *Acta Chem. Scand.*, 48, (1994) 542.
97. F. Rominger, A. Müller and U. Thewalt, *Chem. Ber.*, 127 (1994) 797.
98. S.J. Crimp, L. Spiccia, H.R. Krouse and T.W. Swaddle, *Inorg. Chem.*, 33 (1994) 465.
99. C.P. Rao, S.P. Kaiwar and M.S.S. Raghavan, *Polyhedron*, 13 (1994) 1895.
100. A. Böttcher, H. Elias, J. Glerup, M. Neuburger, C.E. Olsen, J. Springborg, H. Weihe and M. Zehnder, *Acta Chem. Scand.*, 48 (1994) 981.
101. A. Böttcher, H. Elias, J. Glerup, M. Neuburger, C.E. Olsen, J. Springborg, H. Weihe and M. Zehnder, *Acta Chem. Scand.*, 48 (1994) 967.
102. D.B. Dell'amico, F. Calderazzo, F. Gingle, L. Labella and J. Strähle, *Gazz. Chim. Ital.*, 124 (1994) 375.
103. G. Stochel, *Polyhedron*, 13 (1994) 155.
104. A.R.H. Al-Soudani, A.S. Batsanov, P.G. Edwards and J.A.K. Howard, *J. Chem. Soc., Dalton Trans.*, (1994) 987.
105. A. Harton, M.K. Nagi, M.M. Glass, P.C. Junk, J.L. Atwood and J.B. Vincent, *Inorg. Chim. Acta*, 217 (1994) 171.
106. T. Ellis, M. Glass, A. Harton, K. Folting, J.C. Huffman and J.B. Vincent, *Inorg. Chem.*, 33, (1994) 5522.
107. W.Y. Pan and X.F. Yu, *Chin. J. Chem.*, 12 (1994) 534.
108. D.B. Dell'amico, F. Calderazzo, F. Gingle, L. Labella and J. Strähle, *Gazz. Chim. Ital.*, 124 (1994) 375.
109. P. Chaudhuri, F. Birkelbach, M. Winter, V. Staemmler, P. Fleischhauer, W. Haase, U. Flöke and H. J. Haupt, *J. Chem. Soc., Dalton Trans.*, (1994) 2313.
110. Y.M. Shul'ga, I.V. Chernushevich, G.I. Dzhardimalieva, O.S. Roshchupkina, A.F. Dodonov and A.D. Pomogailo, *Izv. Acad. Nauk., Ser. Khim.*, (1994) 1047; English translation: *Russ. Chem. Bull.*, 43 (1994) 983.
111. L. Xu, H. Liu, D. Yan, J. Huang and Q. Zhang, *J. Chem. Soc., Dalton Trans.*, (1994), 2099.
112. J. Glerup, A. Hazell, K. Michelsen and H. Weihe, *Acta Chem. Scand.*, 48 (1994) 618.
113. C.A. Bignozzi, C. Chiorboli, M.T. Indelli, F. Scandola, V. Bertolasi and G. Gilli, *J. Chem. Soc., Dalton Trans.*, (1994), 2391.
114. R. Rominger, A. Müller and U. Thewalt, *Chem. Ber.*, 127 (1994) 797.
115. R.A. Holwerda, *Polyhedron*, 13 (1994) 737.
116. A. Böttcher, H. Elias, J. Glerup, M. Neuburger, C.E. Olsen, J. Springborg, H. Weihe and M. Zehnder, *Acta Chem. Scand.*, 48 (1994) 967.
117. C. Routledge, M. Humanes, Y.J. Li and A.G. Sykes, *J. Chem. Soc., Dalton Trans.*, (1994) 1275.
118. J.B. Vincent, *Inorg. Chem.*, 33, (1994) 5604.
119. P. Spacu, L. Patron, V. Pocol, N. Stanica and D. Crisan, *Rev. Roum. Chim.*, 39 (1994) 1113.
120. C. Rong and F.C. Anson, *Inorg. Chem.*, 33 (1994) 1064.
121. R. Palm and J. Fuchs, *Acta Crystallogr., Sect. C*, C50 (1994) 348.
122. R.D. Archer, A. Lauterbach, and V.O. Ochaya, *Polyhedron*, 13 (1994) 2043.
123. L.F. Larkworthy, G.A. Leonard, D.C. Povey, S.S. Tandon, B.J. Tucker and G.W. Smith, *J. Chem. Soc., Dalton Trans.*, (1994) 1425.
124. F.A. Cotton, L.M. Daniels, L.R. Falvello, C.A. Murillo and A.J. Schultz, *Inorg. Chem.*, 33 (1994) 5396.
125. J.F. Perez-Genito, C. Aria and D. Lamrhari, *New J. Chem.*, 18 (1994) 663.
126. W. Gaede and R. van Eldik, *Inorg. Chem.*, 33 (1994) 2204.
127. N. Shinohara, M. Iwasawa and T. Akiyama, *Bull. Chem. Soc. Jpn.*, 67 (1994) 1033.

128. S. Hao, J. I. Song, H. Aghabozorg and S. Gambarotta, *J. Chem. Soc., Chem. Commun.*, (1994) 157.
129. M.D. Fryzuk, D.B. Leznoff, S.J. Rettig and R.C. Thompson, *Inorg. Chem.*, 33 (1994) 5528.
130. C.S. Alexander and R.J. Balahura, *Inorg. Chem.*, 33 (1994) 1399.
131. M. Shakir, S.P. Varkey and D. Kumar, *Indian J. Chem.*, 33A, (1994) 426.
132. F.A. Cotton, L.M. Daniels, C.A. Murillo and L.A. Zúñiga, *Eur. J. Solid State Inorg. Chem.*, 31 (1994) 535.